

The Hurst roughness exponent and its model-free estimation

Xiyue Han* and Alexander Schied*

November 18, 2021

Abstract

We say that a continuous real-valued function x admits the Hurst roughness exponent H if the p^{th} variation of x converges to zero if $p > 1/H$ and to infinity if $p < 1/H$. For the sample paths of many stochastic processes, such as fractional Brownian motion, the Hurst roughness exponent exists and equals the standard Hurst parameter. In our main result, we provide a mild condition on the Faber–Schauder coefficients of x under which the Hurst roughness exponent exists and is given as the limit of the classical Gladyshev estimates $\hat{H}_n(x)$. This result can be viewed as a strong consistency result for the Gladyshev estimators in an entirely model-free setting, because no assumption whatsoever is made on the possible dynamics of the function x . Nonetheless, our proof is probabilistic and relies on a martingale that is hidden in the Faber–Schauder expansion of x . Since the Gladyshev estimators are not scale-invariant, we construct several scale-invariant estimators that are derived from the sequence $(\hat{H}_n)_{n \in \mathbb{N}}$. We also discuss how a dynamic change in the Hurst roughness parameter of a time series can be detected. Our results are illustrated by means of high-frequency financial time series.

1 Introduction

The Hurst parameter was originally defined by Hurst [13] as a measure of the autocorrelation of a time series. But it is well known that it can also determine the degree of ‘roughness’ of a trajectory, e.g., in terms of the fractal dimension of its graph or its p^{th} variation. Both notions are often used interchangeably in the literature. While the link between autocorrelation and roughness is well-established for stochastic processes such as fractional Brownian motion, it is by no means a universal truth. Indeed, Gneiting and Schlather [10] constructed a class of stationary Gaussian processes for which the Hurst parameter and fractal dimension decouple completely. It is therefore necessary to distinguish between the classical, autocorrelation-based Hurst parameter and a suitable index for the roughness of a trajectory. In this paper, we study such a roughness index, which is based on the p^{th} variation of a continuous real-valued function.

Recall that, if $x : [0, 1] \rightarrow \mathbb{R}$ is a continuous function and $p > 0$, the p^{th} variation of x along the sequence of dyadic partitions is defined as the limit of

$$V_n^{(p)} := \sum_{k=0}^{2^n-1} |x((k+1)2^{-n}) - x(k2^{-n})|^p,$$

*University of Waterloo, 200 University Ave W, Waterloo, Ontario, N2L 3G1, Canada. E-Mails: xiyue.han@uwaterloo.ca, aschied@uwaterloo.ca.

The authors gratefully acknowledge support from the Natural Sciences and Engineering Research Council of Canada through grant RGPIN-2017-04054.

We thank Zhenyuan Zhang for many enlightening discussions.

provided that this limit exists. We will say that x admits the *Hurst roughness exponent* $H > 0$ if

$$\lim_{n \uparrow \infty} V_n^{(p)} = \begin{cases} 0 & \text{for } p > 1/H, \\ \infty & \text{for } p < 1/H. \end{cases} \quad (1.1)$$

Intuitively, the smaller H , the rougher the trajectory x will look. For instance, if x is continuously differentiable, then (1.1) will hold with $H = 1$, and this is also the largest possible value for H unless x is constant. If x is a typical sample path of a continuous semimartingale such as Brownian motion, then (2.2) will hold with $H = 1/2$. If x is a typical sample path of a fractional Brownian motion, then H is equal to its classical Hurst parameter.

When measuring the roughness of a trajectory, there are strong reasons for favouring p^{th} variation over other measures such as fractal dimension. First, the p^{th} variation can be measured in a straightforward manner. Second, other measures may lead to diverging results, and there is no canonical choice. For instance, the graph of a trajectory may have different Hausdorff and box dimensions. Third, and probably most importantly, the p^{th} variation plays a crucial role in the extension of Itô calculus to rough trajectories. A pathwise and strictly model-free version of such an extension for integrators with arbitrary p^{th} variation was recently established by Cont and Perkowski [3]. Itô calculus for rough trajectories also plays an important role in applications, for instance to rough volatility models. These models are based on the observation by Gatheral et al. [8] that the Hurst roughness parameter of the realized volatility of many financial time series is rather small, which makes realized volatility much rougher than the sample paths of Brownian motion.

In Theorem 2.5, our main result, we establish the existence of the Hurst roughness exponent under a mild condition on the Faber–Schauder coefficients of x . We call this condition the reverse Jensen condition and prove that it is satisfied by all typical sample paths of fractional Brownian motion. However, even more important than the existence of the Hurst roughness exponent is the fact that the reverse Jensen condition guarantees that the Hurst roughness exponent of x can be obtained as the limit of the classical Gladyshev estimates $\hat{H}_n(x)$. This part of Theorem 2.5 can be viewed as a strong consistency result for the Gladyshev estimators in an entirely model-free setting, because no assumption whatsoever is made on the possible dynamics of the function x . In particular, we do not assume that x can be obtained as a sample path of some stochastic process. The Gladyshev estimator is derived from the limit theorem developed by Gladyshev [9] and has since been used to estimate the classical Hurst parameter for stochastic processes such as fractional Brownian motion. So one conceptual contribution of Theorem 2.5 is the observation that the Gladyshev estimator actually estimates the Hurst roughness exponent and that its limit only delivers the classical Hurst parameter if and only if the latter coincides with the former.

In Section 3, we discuss the problem of estimating the Hurst roughness exponent from a given continuous function x . For the case in which x is a typical sample path of a stochastic process for which the Hurst roughness exponent is the same as the classical Hurst parameter, we can simply use one of the many estimators for the Hurst parameter available in the literature, and we refer to the book [16] by Kubilius and Mishura for an overview. When estimating the Hurst roughness exponent of a continuous function x in a model-free manner, the fact that the Gladyshev estimator is not scale-invariant becomes an issue. We therefore provide several families of scale-invariant estimators that are derived from the sequence $(\hat{H}_n)_{n \in \mathbb{N}}$. We also relate the estimator used in [8] to those families. Then we discuss how a dynamic change in the Hurst roughness parameter of a time series can be detected. This question is of particular interest in finance, where such a change can signal an alteration in market conditions. We illustrate our corresponding techniques empirically by means of high-frequency financial time series.

While the statement of Theorem 2.5 appears to be completely deterministic, its proof is probabilistic. It relies on martingale techniques that are applied to a martingale that is hidden in the Faber–Schauder

expansion of x . The insights from this probabilistic picture can be used to obtain a number of general mathematical statements on the Hurst roughness parameter of x . These results are stated in Section 4, along with the martingale theory for the Faber–Schauder expansion of a continuous function. We conclude in Section 5. All proofs are collected in Section 6. Finally, the appendices contain extensive summary statistics of our various estimators.

2 The Hurst roughness exponent: definition and a consistency result

Let $x : [0, 1] \rightarrow \mathbb{R}$ be any fixed continuous function. This function could be thought of as a natural or economic time series, a typical sample path of a stochastic process, or a fractal function. What these phenomena have in common is that the corresponding trajectories are not smooth but exhibit a certain degree of ‘roughness’. In the sequel, our goal is to quantify and measure the degree of that roughness. To this end, we will henceforth exclude the trivial case of a constant function x .

For $p > 0$ and $n \in \mathbb{N}$, we define

$$V_n^{(p)} := \sum_{k=0}^{2^n-1} |x((k+1)2^{-n}) - x(k2^{-n})|^p, \quad (2.1)$$

which can be regarded as the p^{th} variation of the function x sampled along the dyadic partition $\{k2^{-n} : k = 0, \dots, 2^n\}$. Suppose that there exists q such that

$$\lim_{n \uparrow \infty} V_n^{(p)} = \begin{cases} 0 & \text{for } p > q, \\ \infty & \text{for } p < q. \end{cases} \quad (2.2)$$

Intuitively, the larger q , the rougher the trajectory x will look. For instance, if x is continuously differentiable, then (2.2) will hold with $q = 1$, and this is also the smallest possible value for q , because x is nonconstant by assumption. If x is a typical sample path of a continuous semimartingale such as Brownian motion, then (2.2) will hold with $q = 2$. More generally, if x is a typical sample path of a fractional Brownian motion with Hurst parameter $H \in (0, 1)$, then q is equal to $1/H$ (see, e.g., [17, Section 1.18]). This analogy motivates the following definition.

Definition 2.1. Suppose that there exists $q \in [1, \infty)$ such that (2.2) holds. Then $H := 1/q$ is called the *Hurst roughness exponent* of $x \in C[0, 1]$.

A concept closely related to the Hurst roughness exponent was used by Gatheral et al. [8] to quantify the roughness of empirical volatility time series. In [19], [12] and [11], the Hurst roughness exponent was computed for certain families of fractal functions. The standard Hurst parameter, on the other hand, is defined via the autocorrelation of the time series and measures the amount of long-range dependence in the data. For many stochastic processes, including fractional Brownian motion, the standard Hurst parameter coincides with the Hurst roughness exponent of the sample paths. In general, however, these two parameters may be different; for a discussion, see Gneiting and Schlather [10], where roughness is measured in terms of fractal dimension.

Remark 2.2. Note that if x admits the Hurst roughness exponent H , then (2.2) does not make any assertion on the existence of $\lim_n V_n^{(p)}$ for $p := 1/H$. This limit always exists for $p = 1$ and is equal to the total variation of x . For $p > 1$, however, the limit may or may not exist. If it does exist, it can be interpreted as the p^{th} variation of the continuous function x along the sequence of dyadic partitions

of $[0, 1]$. This p^{th} variation can be used so as to prove a strictly pathwise version of Itô calculus, an approach that was pioneered by Föllmer [4] for $p \leq 2$ and recently extended to $p > 2$ by Cont and Perkowski [3].

There exist continuous functions that do not admit a Hurst roughness exponent; see [11, Example 3.2]. For this reason, we will first establish criteria for the existence of H . Let us start by defining

$$q^- := \sup \left\{ p > 0 \left| \liminf_{n \uparrow \infty} V_n^{(p)} = \infty \right. \right\} \quad \text{and} \quad q^+ := \sup \left\{ p > 0 \left| \limsup_{n \uparrow \infty} V_n^{(p)} = \infty \right. \right\}.$$

The proof of Proposition 2.3 will show that the following alternative formulas hold for q^- and q^+ ,

$$q^- = \inf \left\{ p \geq 1 \left| \liminf_{n \uparrow \infty} V_n^{(p)} = 0 \right. \right\} \quad \text{and} \quad q^+ = \inf \left\{ p \geq 1 \left| \limsup_{n \uparrow \infty} V_n^{(p)} = 0 \right. \right\}. \quad (2.3)$$

Proposition 2.3. *The Hurst roughness exponent of $x \in C[0, 1]$ exists if and only if $q^+ = q^-$. In this case, $H = 1/q^+ = 1/q^-$.*

Our analysis of the Hurst roughness exponent is based on the Faber-Schauder wavelet expansion of continuous functions. Recall that the *Faber-Schauder functions* are defined as

$$e_\emptyset(t) := t, \quad e_{0,0}(t) := (\min\{t, 1-t\})^+, \quad e_{m,k}(t) := 2^{-m/2} e_{0,0}(2^m t - k)$$

for $t \in \mathbb{R}$, $n \in \mathbb{N}$ and $k \in \mathbb{Z}$. It is well known that the restriction of the Faber-Schauder functions to $[0, 1]$ form a Schauder basis for $C[0, 1]$. More precisely, every function $x \in C[0, 1]$ can be uniquely represented by the following uniformly convergent series,

$$x = x(0) + (x(1) - x(0)) e_\emptyset + \sum_{m=0}^{\infty} \sum_{k=0}^{2^m-1} \theta_{m,k} e_{m,k}. \quad (2.4)$$

where the *Faber-Schauder coefficients* $\theta_{m,k}$ are given by

$$\theta_{m,k} = 2^{m/2} \left(2x\left(\frac{2k+1}{2^{m+1}}\right) - x\left(\frac{k}{2^m}\right) - x\left(\frac{k+1}{2^m}\right) \right).$$

We furthermore denote for $n \in \mathbb{N}$,

$$s_n := \sqrt{\sum_{m=0}^{n-1} \sum_{k=0}^{2^m-1} \theta_{m,k}^2} \quad \text{and} \quad \xi_n := \frac{1}{n} \log_2 s_n. \quad (2.5)$$

Our main thesis in this paper is that the Hurst roughness exponent of x should be equal to the limit of $1 - \xi_n$, provided this limit exists. Theorem 2.5 will rigorously establish this result under the following mild condition on the Faber-Schauder coefficients of x . To formulate this and related conditions, we will say that a function $\varrho : \mathbb{R}_+ \rightarrow \mathbb{R}_+$ is *subexponential* if $\frac{1}{t} \log \varrho(t) \rightarrow 0$ as $t \uparrow \infty$.

Definition 2.4. The Faber-Schauder coefficients of x satisfy the *reverse Jensen condition* if for each $p \geq 1$ there exist $n_p \in \mathbb{N}$ and a non-decreasing subexponential function $\varrho_p : \mathbb{N}_0 \rightarrow [1, \infty)$ such that

$$\frac{1}{\varrho_p(n)} s_n^p \leq \frac{1}{2^{n-1}} \sum_{k=0}^{2^{n-1}-1} \left(\sum_{m=0}^{n-1} 2^m \theta_{m, [2^{m-n+1}k]}^2 \right)^{p/2} \leq \varrho_p(n) s_n^p \quad \text{for } n \geq n_p. \quad (2.6)$$

If $p \geq 2$, then Jensen's inequality implies that the left-hand inequality in (2.6) holds with $\varrho_p = 1$. Likewise, the upper bound holds with $\varrho_p = 1$ if $p \leq 2$. So only the other cases are nontrivial, which explains our terminology “reverse Jensen condition”. As we are going to see in Proposition 2.6, the reverse Jensen condition is satisfied for the typical sample paths of fractional Brownian motion with arbitrary Hurst parameter. Moreover, two alternative conditions that are easier to verify, but are also stronger, will be provided in Proposition 2.7 and an equivalent probabilistic formulation will be given in (4.6). Now we can state our first main result, which establishes the existence of the Hurst roughness parameter and its relation to the limit of the sequence $\xi_n = \frac{1}{n} \log s_n$ under the assumption that the reverse Jensen condition holds.

Theorem 2.5. *Suppose that the Faber–Schauder coefficients of x satisfy the reverse Jensen condition. Then the function x admits the Hurst roughness exponent H if and only if $\xi := \lim_n \log_2 \xi_n$ exists, and in this case we have $H = 1 - \xi$.*

Theorem 2.5 can be regarded as a model-free consistency result for the estimator

$$\hat{H}_n(x) := 1 - \xi_n = 1 - \frac{1}{n} \log_2 s_n \quad (2.7)$$

of the Hurst roughness exponent of the continuous function x . Based on the work by Gladyshev [9], this estimator has been previously considered in the literature and is used for the estimation of the classical Hurst parameter, in particular of Gaussian processes such as fractional Brownian motion. We refer to the book [16] by Kubišius and Mishura for an overview of known results and the related literature. Theorem 2.5, by contrast, is a model-free result because no assumptions are made on x except the reverse Jensen condition. In particular, we do not assume that x is a realization of a stochastic process with prescribed dynamics. Statistical properties of the estimator \hat{H}_n and some improved estimators will be discussed in Section 3.

Theorem 2.5 also shows that the Gladyshev estimator \hat{H}_n from (2.7) is actually an estimator for the Hurst roughness exponent of a continuous function x . Thus, it delivers the classical Hurst parameter if and only if it coincides with the Hurst roughness exponent. This is the case for fractional Brownian motion but, as mentioned above, not universally true. Our next result considers the special situation of fractional Brownian motion and states that all its typical sample paths satisfy the reverse Jensen condition. This result is meant to illustrate the fact that the reverse Jensen condition is a meaningful requirement. Together with Theorem 2.5, it also gives a new proof for the strong consistency of the Gladyshev estimator \hat{H}_n for the special case of fractional Brownian motion.

Proposition 2.6. *With probability one, the sample paths of fractional Brownian motion with arbitrary Hurst parameter $H \in (0, 1)$ satisfy the reverse Jensen condition.*

The following proposition provides two alternative conditions on the Faber–Schauder coefficients of an arbitrary continuous function x that may be easier to verify than the reverse Jensen condition but are also slightly stronger.

Proposition 2.7. *Consider the following two conditions on the Faber–Schauder coefficients of x .*

(a) *There exists a non-decreasing subexponential function γ_1 such that for sufficiently large m ,*

$$\max_{k=0, \dots, 2^m-1} |\theta_{m,k}| \leq \gamma_1(m) \min_{k=0, \dots, 2^m-1} |\theta_{m,k}|.$$

(b) *There exist $\nu \in \mathbb{N}_0$ and a non-decreasing subexponential function $\gamma_2 : \mathbb{N}_0 \rightarrow \mathbb{R}$ such that for sufficiently large $m \geq \nu$,*

$$\max_{k=0, \dots, 2^{m-\nu}-1} \sum_{j=2^\nu k}^{2^\nu(k+1)-1} \theta_{m,j}^2 \leq \gamma_2(m) \min_{k=0, \dots, 2^{m-\nu}-1} \sum_{j=2^\nu k}^{2^\nu(k+1)-1} \theta_{m,j}^2.$$

Then (a) implies (b), and (b) implies the reverse Jensen condition (2.6).

Remark 2.8. Note that Theorem 2.5 could also have been formulated in the following slightly more general form. To this end, suppose that the reverse Jensen condition holds and let us denote

$$\xi^+ := \limsup_{n \uparrow \infty} \log_2 \xi_n \quad \text{and} \quad \xi^- := \liminf_{n \uparrow \infty} \log_2 \xi_n.$$

Then it follows as in the proof of Theorem 2.5 that

$$\limsup_{n \uparrow \infty} V_n^{(p)} = \begin{cases} 0 & \text{if } p > \frac{1}{1-\xi^+}, \\ \infty & \text{if } p < \frac{1}{1-\xi^+}, \end{cases} \quad \liminf_{n \uparrow \infty} V_n^{(p)} = \begin{cases} 0 & \text{if } p > \frac{1}{1-\xi^-}, \\ \infty & \text{if } p < \frac{1}{1-\xi^-}. \end{cases}$$

By (2.2) and (2.3), the Hurst roughness exponent is well defined if and only if $\xi^+ = \xi^-$, and this special case is discussed in Theorem 2.5; on the other hand, if $\xi^+ > \xi^-$, the Hurst roughness exponent does not exist, and the power variation $V_n^{(p)}$ will fluctuate between zero and infinity for any $p \in (1/(1-\xi^-), 1/(1-\xi^+))$.

In Section 4, we will discuss further mathematical properties of the Hurst roughness exponent. We will in particular address properties that can be asserted without assuming the reverse Jensen condition, and we will discuss some probabilistic properties of the p^{th} variation that underlie the proofs of our mathematical results, including Theorem 2.5 and Proposition 2.7.

3 Model-free estimation of the Hurst roughness exponent

In this section, we will introduce and analyze model-free estimators for the Hurst roughness exponent. To this end, recall first from (2.7) that

$$\hat{H}_n(x) = 1 - \xi_n = 1 - \frac{1}{n} \log_2 s_n \tag{3.1}$$

is a consistent estimator for the Hurst roughness exponent of any function $x \in C[0, 1]$ whose Faber–Schauder coefficients $(\theta_{m,k})$ satisfy the reverse Jensen condition. Figure 1 and Table 1 illustrate that the estimator performs very well for sample paths of fractional Brownian motion and yields accurate estimates of the corresponding Hurst parameter.

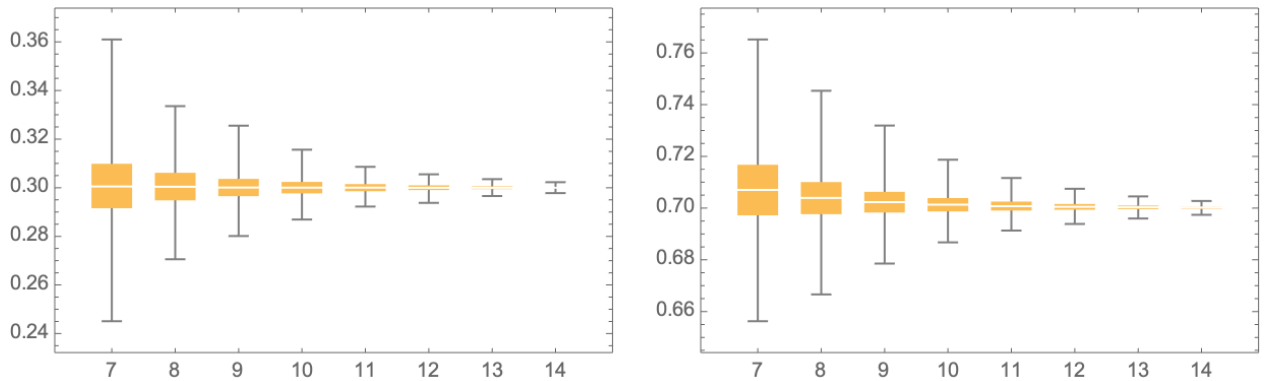


Figure 1: Box plots of \hat{H}_n for $n = 7, \dots, 14$ based on 10,000 sample paths of fractional Brownian motion with $H = 0.3$ (left) and $H = 0.7$ (right).

	Statistics of the estimator \hat{H}_{12}			
	Mean	Standard Deviation	Maximum	Minimum
$H = 0.1$	0.099997	0.00152048	0.106105	0.095413
$H = 0.2$	0.200022	0.00147709	0.204857	0.194787
$H = 0.3$	0.300013	0.00141177	0.304642	0.295447
$H = 0.4$	0.400017	0.00135541	0.404702	0.395667
$H = 0.5$	0.500017	0.00134301	0.504732	0.494933
$H = 0.6$	0.600111	0.00136231	0.605566	0.595617
$H = 0.7$	0.700415	0.00167207	0.705982	0.694329
$H = 0.8$	0.802256	0.00268623	0.810415	0.791342
$H = 0.9$	0.912872	0.00524409	0.930381	0.886319

Table 1: Summary statistics of \hat{H}_{12} applied to 5,000 sample paths of fractional Brownian motion with $H = 0.1, 0.2, \dots, 0.9$.

But the estimator \hat{H}_n also has a disadvantage: it is not scale-invariant. Indeed, we clearly have

$$\hat{H}_n(\lambda x) - \hat{H}_n(x) = -\frac{\log_2 |\lambda|}{n} \quad \text{for } \lambda \neq 0. \quad (3.2)$$

As a consequence, multiplying x with a constant factor can lead to negative or unreasonably large estimates for H and substantially slow down or speed up the convergence $\hat{H}_n(x) \rightarrow H$ (note that both the Hurst roughness exponent itself and the reverse Jensen condition are scale-invariant). Naive normalization of the data does not provide a resolution of this issue, as is illustrated in Figure 2. In the next subsection, we are therefore going to derive intrinsically defined optimal scaling factors and the corresponding improved estimators for the Hurst roughness exponent.

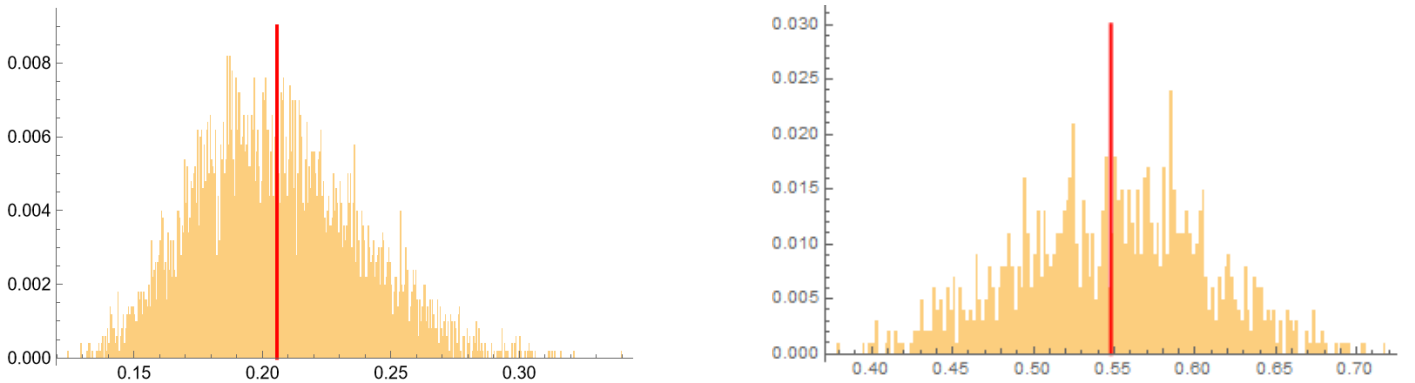


Figure 2: Histograms of \hat{H}_{12} applied to 5000 standardized sample paths of fractional Brownian motion with Hurst parameters $H = 0.3$ (left) and $H = 0.7$ (right). Here, standardization means that each sample path is affinely scaled to have empirical mean zero and variance one. The red vertical lines represent the empirical means of the corresponding estimates.

3.1 Scale-invariant estimators

When presented with a generic time series, we face significant uncertainty about possible data scaling that, as discussed above, can lead to significant underperformance of the estimator \hat{H}_n . In this section,

we will therefore analyze two ideas on constructing scale-invariant estimators for the Hurst roughness exponent out of the sequence (\hat{H}_n) . Both ideas will lead to new estimators that are linear combinations of $\hat{H}_n, \dots, \hat{H}_{n-m}$ for a number m .

The first idea consists in looking for a scaling factor λ_n that optimizes a certain criterion over all possible parameters $\lambda > 0$ and then to take $\hat{H}_n(\lambda_n x)$ as a new estimator. In particular, we will look at the following two choices. A third choice will be given in Definition 3.2.

Definition 3.1. Fix $m \in \mathbb{N}$ and $\alpha_0, \dots, \alpha_m \geq 0$ with $\alpha_0 > 0$.

- (a) For $n > m$, the *sequential scaling factor* λ_n^s and the *sequential scale estimate* $H_n^s(x)$ are defined as follows,

$$\lambda_n^s := \arg \min_{\lambda > 0} \sum_{k=n-m}^n \alpha_{n-k} \left(\hat{H}_k(\lambda x) - \hat{H}_{k-1}(\lambda x) \right)^2 \quad \text{and} \quad H_n^s(x) := \hat{H}_n(\lambda_n^s x). \quad (3.3)$$

The corresponding mapping $H_n^s : C[0, 1] \rightarrow \mathbb{R}$ will be called the *sequential scale estimator*.

- (b) The *terminal scaling factor* λ_n^t and the *terminal scale estimate* $H_n^t(x)$ are defined as follows,

$$\lambda_n^t := \arg \min_{\lambda > 0} \sum_{k=n-m}^n \alpha_{n-k} \left(\hat{H}_n(\lambda x) - \hat{H}_{k-1}(\lambda x) \right)^2, \quad \text{and} \quad H_n^t(x) := \hat{H}_n(\lambda_n^t x). \quad (3.4)$$

The corresponding mapping $H_n^t : C[0, 1] \rightarrow \mathbb{R}$ will be called the *terminal scale estimator*.

We will see in Theorem 3.3 that Definition 3.1 is well posed, because the minimization problems in (3.3) and (3.4) admit unique solutions for every function $x \in C[0, 1]$. The intuition for sequential scaling is fairly simple. The sequential scaling factor λ_n^s minimizes the weighted mean-squared differences $\hat{H}_k(\lambda x) - \hat{H}_{k-1}(\lambda x)$ for $k = m+1, \dots, n$. Since \hat{H}_n is a consistent estimator, the faster the sequence $\hat{H}_k(\lambda x)$ converges, the more accurate the final estimate $\hat{H}_n(\lambda x)$ will be. The idea for terminal scaling is also straightforward: Since the estimator \hat{H}_n is consistent, the last estimate $\hat{H}_n(x)$ should be more precise than any other previous value $\hat{H}_k(x)$ with $k < n$. Therefore, we aim at minimizing the weighted mean-squared differences $\hat{H}_k(\lambda x)$ and $\hat{H}_n(\lambda x)$.

Our second idea for constructing a scale-invariant estimator is as follows. It follows from (3.2) that for $\lambda > 0$

$$n\hat{H}_n(x) = n\hat{H}_n(\lambda x) + \log_2 \lambda.$$

For an ideal scaling factor λ , the right-hand side will be close to $nH + \log_2 |\lambda|$. Therefore, the idea is to perform linear regression on the data points $(n-m)\hat{H}_{n-m}(x), (n-m-1)\hat{H}_{n-m-1}(x), \dots, n\hat{H}_n(x)$ and to take the corresponding slope as an estimator for H .

Definition 3.2. Let $m \in \mathbb{N}$ and $\alpha_0, \dots, \alpha_m \geq 0$ be such that $\sum_{k=0}^m \alpha_k = 1$. Then, for $n > m$, the *regression scale estimate* $H_n^r(x)$ and the *regression scaling factor* λ_n^r are given by

$$(H_n^r(x), \lambda_n^r) = \arg \min_{h \in \mathbb{R}, \lambda > 0} \sum_{k=0}^m \alpha_k \left((n-k)(\hat{H}_{n-k}(x) - h) - \log_2 \lambda \right)^2. \quad (3.5)$$

The corresponding mapping $H_n^r : C[0, 1] \rightarrow \mathbb{R}$ will be called the *regression scale estimator*.

The next theorem shows in particular that all three estimators can be represented by linear combinations of the estimators \hat{H}_k for $m \leq k \leq n$ and that they are scale-invariant estimators of the Hurst roughness exponent H . Summary statistics of our scale estimators can be found in Appendix A.

Theorem 3.3. Consider the context of Definitions 3.1 and 3.2 with fixed $m \in \mathbb{N}$ and $\alpha_0, \dots, \alpha_m \geq 0$ such that $\alpha_0 > 0$.

- (a) The three optimization problems in (3.3), (3.4), and (3.5) admit unique solutions for every function $x \in C[0, 1]$. In particular, all objects in Definitions 3.1 and 3.2 are well defined.
- (b) The sequential and terminal scale estimators can be represented by the following respective linear combinations of the estimators \hat{H}_k ,

$$H_n^s = \beta_{n,n} \hat{H}_n + \dots + \beta_{n,n-m-1} \hat{H}_{n-m-1} \quad \text{and} \quad H_n^t = \gamma_{n,n} \hat{H}_n + \dots + \gamma_{n,n-m-1} \hat{H}_{n-m-1}$$

where

$$\beta_{n,k} = \begin{cases} 1 + \frac{\alpha_0}{c_n^s n^2 (n-1)} & \text{if } k = n, \\ \frac{1}{c_n^s n k} \left(\frac{\alpha_{n-k}}{k-1} - \frac{\alpha_{n-k-1}}{k+1} \right) & \text{if } n-m \leq k \leq n-1, \\ \frac{-\alpha_m}{c_n^s n (n-m)(n-m-1)} & \text{if } k = n-m-1, \end{cases} \quad \text{for } c_n^s := \sum_{k=n-m}^n \frac{\alpha_{n-k}}{k^2 (k-1)^2},$$

and

$$\gamma_{n,k} = \begin{cases} 1 + \frac{1}{c_n^t n^2} \sum_{j=n-m}^n \alpha_{n-j} \frac{n-j+1}{j-1} & \text{if } k = n, \\ \frac{k-n}{c_n^t n^2 k} \alpha_{n-k+1} & \text{otherwise,} \end{cases} \quad \text{for } c_n^t = \sum_{k=n-m}^n \alpha_{n-k} \left(\frac{n-k+1}{n(k-1)} \right)^2.$$

If in addition $\sum_k \alpha_k = 1$, then the regression scale estimator is given by

$$H_n^r = \frac{1}{c^r} \sum_{k=0}^m \alpha_k (n-k)(k-a) \hat{H}_{n-k}, \quad \text{where } a = \sum_{k=0}^m \alpha_k k \text{ and } c^r = a^2 - \sum_{k=0}^m \alpha_k k^2. \quad (3.6)$$

- (c) The sequential, terminal, and regression scale estimators are scale-invariant. That is, for $n > m$, $x \in C[0, 1]$, and $\lambda \neq 0$, we have $H_n^t(\lambda x) = H_n^t(x)$, $H_n^s(\lambda x) = H_n^s(x)$ and $H_n^r(\lambda x) = H_n^r(x)$.
- (d) If $x \in C[0, 1]$ is such that $|\hat{H}_n(x) - H| = O(a_n)$ as $n \uparrow \infty$ for some sequence $a_n \searrow 0$, then $|H_n^s(x) - H| = |H_n^t(x) - H| = |H_n^r(x) - H| = O(na_n)$.

Remark 3.4. Part (d) of Theorem 3.3 implies in particular the consistency of the sequential, terminal, and regression scale estimators if $x \in C[0, 1]$ satisfies $|\hat{H}_n(x) - H| = o(1/n)$. According to Theorem 1 in [15] and [14], the typical sample paths of fractional Brownian motion B^H with Hurst parameter $H \in (1/2, 1)$ satisfy $|\hat{H}_n(B^H) - H| = O(n2^{-(2-2H)n})$. Hence, our scale estimators are also consistent in this setup and of rate $O(n2^{-(2-2H)n})$.

Remark 3.5. A general scale-invariant estimator can be constructed by solving an optimization problem of the form

$$\tilde{\lambda} := \arg \min_{\lambda > 0} \sum_{j > k}^n \alpha_{j,k} |\hat{H}_j(\lambda x) - \hat{H}_k(\lambda x)|^2,$$

where $\alpha_{j,k}$ are given coefficients, and by setting $\tilde{H}_n(x) := \hat{H}_n(\tilde{\lambda} x)$. If the global minimizer $\tilde{\lambda}$ exists, the estimate $\tilde{H}_n(x)$ will be a linear combination of the estimates $\hat{H}_k(x)$.

Let us now investigate the relations between our estimators and the one used in [8]. To this end, we let for $x \in C[0, 1]$, $n, k \in \mathbb{N}$ and $q \in \mathbb{R}^+$,

$$m(q, k, n) := \left\lfloor \frac{k}{2^n} \right\rfloor^{-1} \sum_{j=1}^{\lfloor 2^n/k \rfloor} |x(kj2^{-n}) - x(k(j-1)2^{-n})|^q.$$

Following Rosenbaum [22], Gatheral et al. [8] assume that there exists a positive constant b_q such that

$$(k2^{-n})^{-qH} m(q, k, n) \rightarrow b_q, \quad \text{for any fixed } k \in \mathbb{N}, \text{ as } n \uparrow \infty,$$

From here, the estimator H_n^v from [8] is computed by way of a linear regression. More precisely, let \mathcal{K} be a finite collection of positive integers and \mathcal{Q} be a finite collection of positive real numbers. For $q \in \mathcal{Q}$, the estimate $H_{n,q}^v(x)$ of the Hurst roughness exponent of the continuous function x using the q^{th} variation is obtained by regressing $\log m(q, k, n)$ with respect to $\log k$, i.e.,

$$(H_{n,q}^v(x), b_q) = \arg \min_{h \in \mathbb{R}, b_q > 0} \sum_{k \in \mathcal{K}} \left(\log_2 m(q, k, n) - \log_2 b_q - qh(\log_2 k - n) \right)^2. \quad (3.7)$$

Standard computations for linear regression then yield that

$$H_{n,q}^v(x) = \frac{\sum_{k \in \mathcal{K}} (\log k - \overline{\log \mathcal{K}}) (\log m(q, k, n) - \overline{\log m(q, \mathcal{K}, n)})}{q \cdot \sum_{k \in \mathcal{K}} (\log k - \overline{\log \mathcal{K}})},$$

where $|\cdot|$ denotes the cardinality of a set and

$$\overline{\log \mathcal{K}} = \frac{1}{|\mathcal{K}|} \sum_{k \in \mathcal{K}} \log k \quad \text{and} \quad \overline{\log m(q, \mathcal{K}, n)} = \frac{1}{|\mathcal{K}|} \sum_{k \in \mathcal{K}} \log m(q, k, n).$$

The *simple regression estimate* $H_n^v(x)$ is then the sample average of $H_{n,q}^v(x)$ for all $q \in \mathcal{Q}$. In other words, we have

$$H_n^v(x) := \frac{1}{|\mathcal{Q}|} \sum_{q \in \mathcal{Q}} H_{n,q}^v(x).$$

The corresponding mapping $H_n^v : C[0, 1] \rightarrow \mathbb{R}$ will be called the *simple regression estimator*, which is a formal description of the estimator used in [8]. It is also clear that the simple regression estimator H_n^v is scale-invariant, i.e., for any $n \in \mathbb{N}$ and $x \in C[0, 1]$, we have $H_n^v(\lambda x) = H_n^v(x)$ for any $\lambda \neq 0$. Our next result states that it is a particular case of our regression scale estimator under a certain choice of parameters.

Proposition 3.6. *Let $\mathcal{Q} = \{2\}$, $\mathcal{K} = \{1, 2, \dots, 2^m\}$ and $\alpha_k = \alpha$ for all k and some $\alpha > 0$. Then the regression scale estimator H_n^r coincides with the simple regression estimator H_n^v for all $n > m$.*

3.2 Detecting changes of the Hurst exponent on a long time series

In many applications, dynamically monitoring the Hurst (roughness) exponent of a time series is important. An example is the ExtremeHurstTM function on Bloomberg, which can be used for market timing. For dynamic monitoring, the original time series is divided into several (possibly overlapping) intervals, and the Hurst (roughness) exponent is then measured on each of these intervals.

For a formal description, we fix $x \in C[0, T]$ and an interval shift $0 \leq \tau \leq T - 1$. Then we let $x_\tau(t) := x(t + \tau)$ for $t \in [0, 1]$. For any estimator \hat{H} , the value $\hat{H}(x_\tau)$ gives an estimate of Hurst roughness exponent of x over the interval $[\tau, \tau + 1]$.

Definition 3.7. Let $x \in C[0, T]$ and $\mathbb{T} := \{0 \leq \tau_1 < \tau_2 < \dots < \tau_N \leq T - 1\}$. Fix $m \in \mathbb{N}$ and $\alpha_0, \dots, \alpha_m \geq 0$ with $\alpha_0 > 0$.

- (a) For $n > m$, the \mathbb{T} -adjusted sequential scaling factor $\lambda_n^{s, \mathbb{T}}$ and the \mathbb{T} -adjusted sequential scale estimate $H_n^{s, \mathbb{T}}(x)$ are defined as follows,

$$\lambda_n^{s, \mathbb{T}} := \arg \min_{\lambda > 0} \sum_{j=1}^N \sum_{k=n-m}^n \alpha_{n-k} \left(\widehat{H}_k(\lambda x_{\tau_j}) - \widehat{H}_{k-1}(\lambda x_{\tau_j}) \right)^2 \quad \text{and} \quad H_n^{s, \mathbb{T}}(x) := \widehat{H}_n(\lambda_n^{s, \mathbb{T}} x). \quad (3.8)$$

The corresponding mapping $H_n^{s, \mathbb{T}} : C[0, 1] \rightarrow \mathbb{R}$ will be called the (\mathbb{T} -adjusted) sequential scale estimator.

- (b) For $n > m$, the terminal scaling factor $\lambda_n^{t, \mathbb{T}}$ and the \mathbb{T} -adjusted terminal scale estimate $H_n^{t, \mathbb{T}}(x)$ are defined as follows,

$$\lambda_n^{t, \mathbb{T}} := \arg \min_{\lambda > 0} \sum_{j=1}^N \sum_{k=n-m}^n \alpha_{n-k} \left(\widehat{H}_n(\lambda x_{\tau_j}) - \widehat{H}_{k-1}(\lambda x_{\tau_j}) \right)^2 \quad \text{and} \quad H_n^{t, \mathbb{T}}(x) := \widehat{H}_n(\lambda_n^{t, \mathbb{T}} x). \quad (3.9)$$

The corresponding mapping $H_n^{t, \mathbb{T}} : C[0, 1] \rightarrow \mathbb{R}$ will be called the (\mathbb{T} -adjusted) terminal scale estimator.

In many applications, dynamically monitoring the Hurst (roughness) exponent of a time series is important. An example is the ExtremeHurstTM function on Bloomberg, which can be used for market timing. For dynamic monitoring, the original time series is divided into several (possibly overlapping) intervals, and the Hurst (roughness) exponent is then measured on each of these intervals.

For a formal description, we fix $x \in C[0, T]$ and an interval shift $0 \leq \tau \leq T - 1$. Then we let $x_\tau(t) := x(t + \tau)$ for $t \in [0, 1]$. For any estimator \widehat{H} , the value $\widehat{H}(x_\tau)$ gives an estimate of Hurst roughness exponent of x over the interval $[\tau, \tau + 1]$.

Theorem 3.8. Consider the context of Definitions 3.7 with fixed $m \in \mathbb{N}$ and $\alpha_0, \dots, \alpha_m \geq 0$ such that $\alpha_0 > 0$.

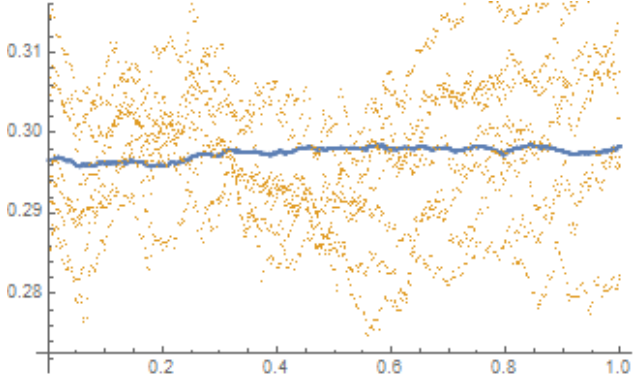
- (a) The two optimization problems in (3.8) and (3.9) admit unique solutions for every function $x \in C[0, 1]$. In particular, all objects in Definitions 3.7 are well defined.
- (b) The \mathbb{T} -adjusted sequential scaling factor and scale estimate can be represented as follows:

$$\log_2 \lambda_n^{s, \mathbb{T}} = \frac{1}{N} \sum_{j=1}^N \log_2 \lambda_n^{s, \{\tau_j\}} \quad \text{and} \quad H_n^{s, \mathbb{T}} = \widehat{H}_n + \frac{1}{N} \sum_{j=1}^N \left(H_n^{s, \{\tau_j\}}(x_{\tau_j}) - \widehat{H}_n(x_{\tau_j}) \right),$$

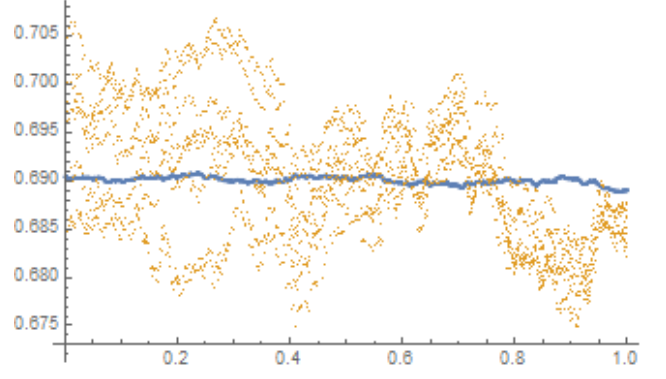
Moreover, the same representations hold if we replace the sequential factor/estimate/estimator to terminal factor/estimate/estimator.

- (c) The sequential and terminal scale estimators are scale-invariant. That is, for $n > m$, $x \in C[0, T]$, and $\lambda \neq 0$, we have $H_n^{t, \mathbb{T}}(\lambda x_\tau) = H_n^{t, \mathbb{T}}(x_\tau)$ and $H_n^{s, \mathbb{T}}(\lambda x_\tau) = H_n^{s, \mathbb{T}}(x_\tau)$.

The following figure illustrates that applying the \mathbb{T} -adjusted scale estimator significantly reduces the fluctuation of the scale estimates over a sequence of intervals compared with a direct application of corresponding estimators. This also results in a smooth curve of the estimated Hurst parameter over time.



$H = 0.3$



$H = 0.7$

Figure 3: Plots of terminal scale estimates $H_n^{t, \mathbb{T}}(x_\tau)$ (in blue) and $H_n^{t, \{\tau\}}(x_\tau)$ (in yellow) for $\tau \in \{k2^{-14} | k = 0, 1, \dots, 2^{14}\}$ applied to a single trajectory of fractional Brownian motion. The other parameters are chosen to be $m = 3$, $n = 14$, $\alpha_k = 1$ and $\mathbb{T} = \{k2^{-14} | k = 0, 1, \dots, 2^{14}\}$.

In the sequel, we apply the \mathbb{T} -adjusted terminal scale estimator to estimate the roughness of certain high-frequency financial time series. We implement our estimator with $n = 11$, $m = 1$ and $\alpha_k = 2^{-k}$ based on 5-minute data and rolling estimation intervals, each with previous $2^{11} + 1$ data points, i.e., 7.11 days $= 2^{11} \times 5$ minutes. Furthermore, we set \mathbb{T} to be the collection of all data points. We plot the estimates of the Hurst roughness exponent in blue and the futures price in orange over time.

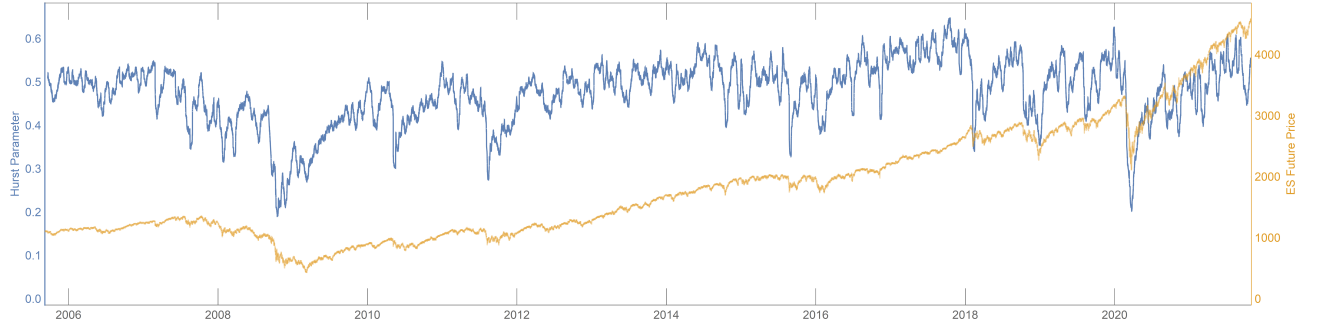


Figure 4: Plot of the Hurst roughness exponent (blue) for e-mini SPX futures (ES, orange), estimated by $H_n^{t, \mathbb{T}}$ with $n = 11$, $m = 1$ and $\alpha_k = 2^{-k}$.

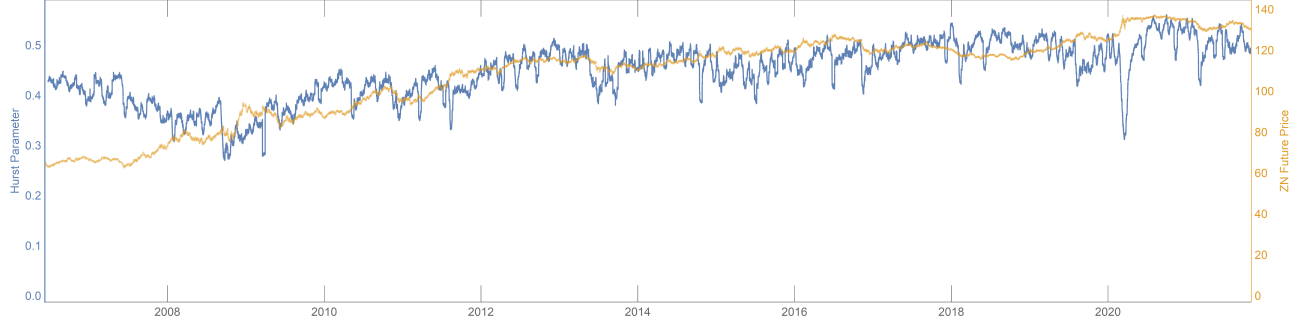


Figure 5: Plot of the Hurst roughness exponent (blue) for 10-year treasury note futures (ZN, orange), estimated by $H_n^{t,\mathbb{T}}$ with $n = 11$, $m = 1$ and $\alpha_k = 2^{-k}$.

As one can see from Figure 4 and Figure 5, the Hurst roughness exponent stays around 0.5 most of the time. The market thus exhibits diffusive behavior, which is consistent with the arbitrage requirement of finite and non-vanishing quadratic variation observed by Föllmer [5] (see also [6] and Proposition 2.1 in [23] for extensions of this argument). Exceptions to this behavior, however, tend to occur during market crises, during which we observe a positive correlation between futures prices and their Hurst roughness exponent. In Figure 6, we focus on the 2008 financial crisis, and the summary statistics can be found in Appendix B.

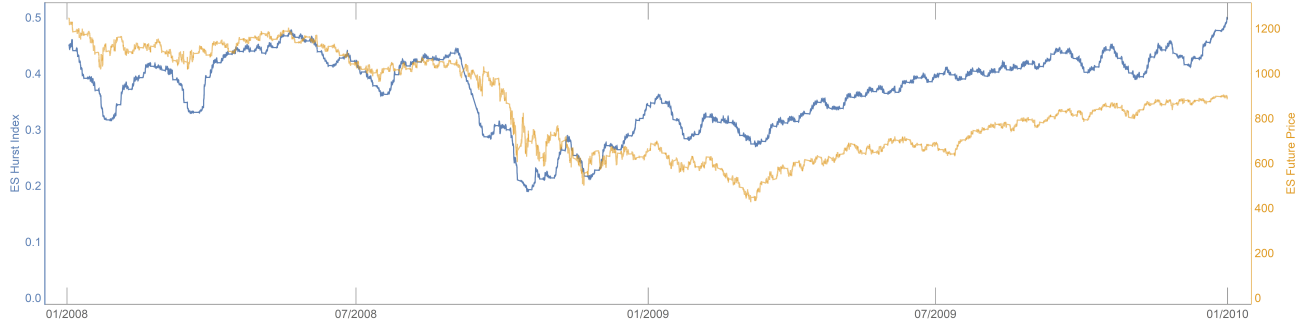


Figure 6: Plot of the Hurst roughness exponent (blue) for e-mini SPX futures (ES, orange) during 2008 and 2009, estimated by $H_n^{t,\mathbb{T}}$ with $n = 11$, $m = 1$ and $\alpha_k = 2^{-k}$.

Next, we consider the roughness of the realized volatility of the SPX index. Gatheral et al. [8] split the volatility process into halves and estimate the Hurst parameter of each separated process. Based on their numerical results, they claim that the Hurst parameter does not vary remarkably over time. We proxy the realized volatility by the daily realized volatility estimates from the Oxford-Man Institute of Quantitative Finance Realized Library (from Jan 03, 2000 to Nov 15, 2021) and apply the terminal \mathbb{T} -adjusted scale estimator to estimate the degree of smoothness of the log volatility. We implement our estimation with $m = 1$ and $\alpha_k = 2^{-k}$ based on daily data and rolling estimation intervals, each

with previous $2^n + 1$ data points, i.e., 2^n days for $n = 8$ (approx. 1 year) and $n = 10$ (approx. 4 years). Furthermore, we set \mathbb{T} to be the collection of all data points.

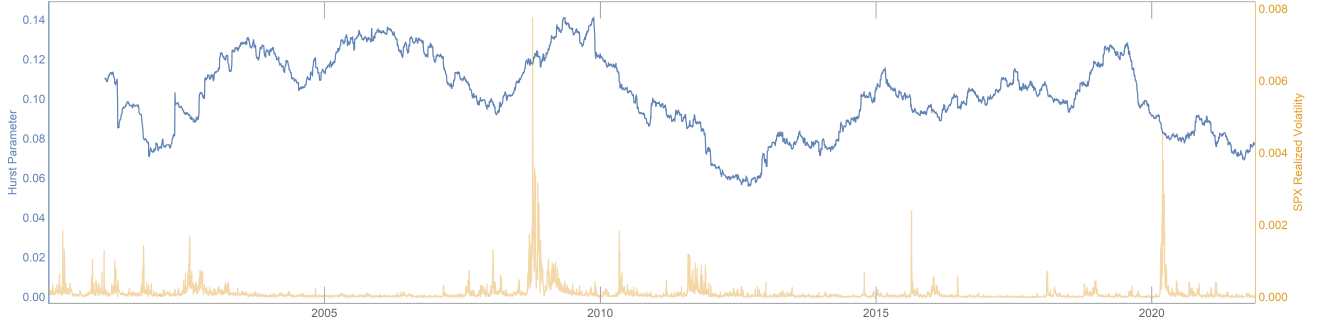


Figure 7: Plot of the Hurst roughness exponent (blue) for the log volatility of the SPX index (orange), estimated by $H_n^{t,\mathbb{T}}$ with $n = 8$, $m = 1$ and $\alpha_k = 2^{-k}$.

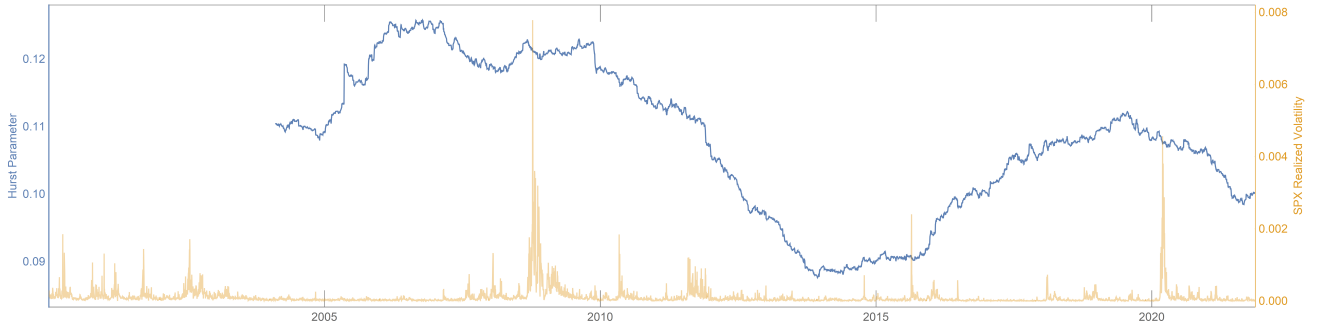


Figure 8: Plot of the Hurst roughness exponent (blue) for the log volatility of the SPX index (orange), estimated by $H_n^{t,\mathbb{T}}$ with $n = 10$, $m = 1$ and $\alpha_k = 2^{-k}$.

We can notice from the above plots that even though different estimation intervals will alter the shape of the curve of the Hurst roughness exponent, all the estimated Hurst roughness exponents are located around 0.1. This, together with, summary statistics in Appendix C confirms the claim in [8].

4 General properties of the Hurst roughness exponent

In this section, we collect some general mathematical properties of the Hurst roughness exponent. As in Section 2, we fix an arbitrary function $x \in C[0, 1]$ with Faber-Schauder coefficients $(\theta_{m,k})$ and quantities s_n and $\xi_n = \frac{1}{n} \log_2 s_n$ as defined in (2.5), but we do not assume that the reverse Jensen condition is satisfied. Recall from Theorem 2.5 that this condition guarantees the existence of the Hurst roughness exponent H of x if and only if $\xi = \lim_n \xi_n$ exists and that in this case $H = 1 - \xi$. The following

results summarize what can be stated without assuming the reverse Jensen condition. We start with the following a priori estimates linking H and ξ .

Proposition 4.1. *Suppose that x admits the Hurst roughness exponent H , and $\xi = \lim_n \xi_n$ exists. Then the following assertions hold:*

- (a) *If $\xi > 1/2$, then $H \leq 1/2$; if $\xi < 1/2$, then $H \geq 1/2$.*
- (b) *If $H \leq 1/2$, then $H \leq 1 - \xi$.*
- (c) *If $H \geq 1/2$, then $H \geq 1 - \xi$.*

The preceding proposition provides one-sided bounds on the Hurst roughness exponent in terms of ξ . Our next result gives universal two-sided bounds for H . To this end, for $m \in \mathbb{N}$, we denote by

$$\widehat{F}_m(t) := 2^{-m} \left(\sum_{k=0}^{2^m-1} \mathbb{1}_{\{\theta_{m,k}^2 \leq t 2^{-m}\}} \right)$$

the empirical distribution of the m^{th} generation Faber-Schauder coefficients and let \widehat{F}_m^{-1} be a corresponding quantile function.

Proposition 4.2. *Suppose that x admits the Hurst roughness exponent H . We define for $\nu \in \mathbb{N}$ and $n \in \mathbb{N}$,*

$$\begin{aligned} \xi_{\nu,n}^- &:= \frac{1}{2n} \log_2 \sum_{m=0}^{n-1} \frac{1}{m^\nu} \sum_{k=1}^{m^\nu} \widehat{F}_m^{-1} \left(2^{-m} \left\lfloor \frac{2^m(k-1)}{m^\nu} \right\rfloor \right), \\ \xi_{\nu,n}^+ &:= \frac{1}{2n} \log_2 \sum_{m=0}^{n-1} \frac{1}{m^\nu} \sum_{k=1}^{m^\nu} \widehat{F}_m^{-1} \left(2^{-m} \left\lceil \frac{2^m k}{m^\nu} \right\rceil \right). \end{aligned}$$

If the limits $\xi_\nu^\pm := \lim_{n \uparrow \infty} \xi_{\nu,n}^\pm$ exist for some $\nu \in \mathbb{N}$, then $1 - \xi_\nu^+ \leq H \leq 1 - \xi_\nu^-$.

Our next result looks at the special case of functions x of bounded variation. Such functions clearly have the Hurst roughness exponent $H = 1$. The converse statement, however, is not true: there exist functions with $H = 1$ that are nowhere differentiable and hence not of bounded variation. One such example is the classical Takagi function; see Remark 2.2 (i) in [24] for details. In our general context, where we fix an arbitrary function $x \in C[0, 1]$ with Faber-Schauder coefficients $(\theta_{m,k})$ and quantities s_n and ξ_n given by (2.5), we have the following result.

Proposition 4.3. *The following assertions hold:*

- (a) *If $\sup_n s_n < \infty$, then the function x is of bounded variation.*
- (b) *If the function x is of bounded variation, then $\sup_n 2^{-n/2} \sum_{k=0}^{2^n-1} |\theta_{n,k}| < \infty$.*

We continue this section with a comparison result for the Hurst roughness exponents of two continuous functions $x, y \in C[0, 1]$ with respective Faber-Schauder coefficients $(\theta_{m,k})$ and $(\mu_{m,k})$.

Proposition 4.4. *Suppose that there exists $\nu \in \mathbb{N}$ such that $|\theta_{m,k}| = |\mu_{m,k}|$ for $m \geq \nu$ and $k \leq 2^m - 1$. Then the function x admits the Hurst roughness exponent H if and only if the function y admits the Hurst roughness exponent H .*

The following proposition considers the Hurst roughness exponent of the sum, $x + y$, of two continuous functions x and y . By taking $y = -x$, we see that the sum can be arbitrarily smooth, so a condition will be needed so as to obtain a nontrivial result. Our condition will be the following:

$$\text{There exists } \nu \in \mathbb{N} \text{ such that } \text{sign}(\theta_{m,k}) = \text{sign}(\mu_{m,k}) \text{ for } m \geq \nu \text{ and } k \leq 2^m - 1, \quad (4.1)$$

where $(\theta_{m,k})$ and $(\mu_{m,k})$ are the Faber–Schauder coefficients of the respective functions x and y .

Proposition 4.5. *Suppose that $x, y \in C[0, 1]$ admit the Hurst roughness exponents H_x and H_y and (4.1) holds. Then the function $x + y$ admits the Hurst roughness exponent $\min(H_x, H_y)$.*

We end this section with a preview of our proof method, as it might be of some independent interest. This method relies on martingale techniques and further develops the probabilistic approach to the p^{th} variation of fractal functions that goes back to [19, 24]. Let $(\Omega, \mathcal{F}, \mathbb{P})$ be a probability space supporting an i.i.d. sequence $(U_n)_{n \in \mathbb{N}}$ of $\{0, 1\}$ -valued random variables with symmetric Bernoulli distribution. Furthermore, we define the stochastic processes

$$R_0 := 0, \quad R_m := \sum_{k=1}^m 2^{-k} U_k \quad \text{and} \quad S_m := 2^m \theta_{m, 2^m R_m}^2, \quad m \in \mathbb{N}_0. \quad (4.2)$$

Note that R_m is uniformly distributed on $\{k 2^{-m} : k = 0, \dots, 2^m - 1\}$. The link between these stochastic processes and the quantities $V_n^{(p)}$ is established in the following proposition, which is based on Burkholder’s martingale inequality and which provides the key to the entire analysis in this paper.

Proposition 4.6. *Suppose that $x(0) = x(1) = 0$. Then, for $p \geq 1$, there exist constants $0 < A_p \leq B_p < \infty$ depending only on p but not on x , such that for all $n \in \mathbb{N}$,*

$$A_p 2^{n(1-p)} \mathbb{E} \left[\left(\sum_{m=0}^{n-1} S_m \right)^{p/2} \right] \leq V_n^{(p)} \leq B_p 2^{n(1-p)} \mathbb{E} \left[\left(\sum_{m=0}^{n-1} S_m \right)^{p/2} \right]. \quad (4.3)$$

Moreover, in the special case $p = 2$, we have

$$V_n^{(2)} = 2^{-n} s_n^2. \quad (4.4)$$

Note that

$$\mathbb{E} \left[\sum_{m=0}^{n-1} S_m \right] = s_n^2 \quad \text{and} \quad \mathbb{E} \left[\left(\sum_{m=0}^{n-1} S_m \right)^{p/2} \right] = \frac{1}{2^{n-1}} \sum_{k=0}^{2^{n-1}-1} \left(\sum_{m=0}^{n-1} 2^m \theta_{m, \lfloor 2^{m-n+1} k \rfloor}^2 \right)^{p/2}. \quad (4.5)$$

We can thus rephrase the reverse Jensen condition as follows: there exist $n_p \in \mathbb{N}$ and a non-decreasing subexponential function $\varrho_p : \mathbb{N}_0 \rightarrow [1, \infty)$ such that

$$\frac{1}{\varrho_p(n)} \mathbb{E} \left[\sum_{m=0}^{n-1} S_m \right]^{p/2} \leq \mathbb{E} \left[\left(\sum_{m=0}^{n-1} S_m \right)^{p/2} \right] \leq \varrho_p(n) \mathbb{E} \left[\sum_{m=0}^{n-1} S_m \right]^{p/2} \quad \text{for } n \geq n_p. \quad (4.6)$$

5 Conclusion and outlook

In this paper, we have developed a general theory of the Hurst roughness exponent of a continuous function x . Our main result provides a mild condition on the Faber–Schauder coefficients of x under which the Hurst roughness exponent exists and is given as the limit of the Gladyshev estimates $\hat{H}_n(x)$.

We have then derived scale-invariant estimators, which are strongly consistent as soon as the convergence of $\hat{H}_n(x)$ is of the order $o(1/n)$. We also considered the problem of detecting dynamic changes of the Hurst roughness in a long time series and applied our techniques to high-frequency financial time series.

A possible direction of future research concerns an extension of our theory to data that are unequally spaced. In this case, the standard Faber–Schauder expansion can no longer be applied. It might be interesting to see, though, if the techniques developed by Cont and Das [1, 2] can be set to work here.

6 Proofs

6.1 Proofs for the results in Section 2 and 4

Proof of Proposition 2.3. The assertion follows easily from the alternative representation (2.3) of q^- and q^+ , so it is sufficient to establish (2.3). To prove this result for q^- , let

$$q_0 := \inf \left\{ p \geq 1 \mid \liminf_{n \uparrow \infty} V_n^{(p)} = 0 \right\}.$$

Let n_0 be such that $\max_k |x((k+1)2^{-n}) - x(k2^{-n})| \leq 1$ for $n \geq n_0$. Then $p \mapsto V_n^{(p)}$ is non-increasing for $n \geq n_0$, and so we must have $q^- \leq q_0$. To show the converse inequality, we show that $\liminf_n V_n^{(p)} = 0$ for every $p > q^-$. To this end, we assume by way of contradiction that there exists $p > q^-$ such that $v := \liminf_n V_n^{(p)} > 0$. The definition of q^- implies that we must have $v < \infty$. Next, for any $\varepsilon > 0$, there exists $n_1 \in \mathbb{N}$ such that $\max_k |x((k+1)2^{-n}) - x(k2^{-n})| \leq \varepsilon$ for $n \geq n_1$. Thus, for $q \in (q^-, p)$ and $n \geq n_1$,

$$V_n^{(p)} \leq \max_k |x((k+1)2^{-n}) - x(k2^{-n})|^{p-q} \cdot V_n^{(q)} \leq \varepsilon^{p-q} V_n^{(q)}.$$

When sending $\varepsilon \downarrow 0$, we see that $0 < v \leq \varepsilon^{p-q} \liminf_n V_n^{(q)}$ for all $\varepsilon > 0$. This implies that $\liminf_n V_n^{(q)} = \infty$, which, in view of $q > q^-$, contradicts the definition of q^- . This establishes $q_0 = q^-$. The second identity in (2.3) is proved in the same manner. \square

Proof of Proposition 2.7. (a) \Rightarrow (b): If condition (a) holds, then (b) holds with $\nu = 0$ and $\gamma_2 = \gamma_1^2$.

(b) \Rightarrow (2.6): For the ease of notation, we prove this implication only for the case $\nu = 1$; the case $\nu \geq 2$ can be proved analogously. Recall that the upper bound in the reverse Jensen condition holds with $\varrho_p \equiv 1$ if $q := p/2 \leq 1$. So it is sufficient to deduce this upper bound for $q > 1$. We will use the probabilistic formalism introduced in (4.2). Note first that

$$\frac{1}{2^{n-1}} \sum_{k=0}^{2^{n-1}-1} \left(\sum_{m=0}^{n-1} 2^m \theta_{m, \lfloor 2^{m-n} k \rfloor}^2 \right)^{p/2} = \mathbb{E} \left[\left(\sum_{m=0}^{n-1} S_m \right)^q \right].$$

Let $a_0, \dots, a_{n-1} \geq 0$ and note that $(\sum_i a_i)^q \leq n^{q-1} \sum_i a_i^q$ by Jensen's inequality. Hence,

$$\begin{aligned} \mathbb{E} \left[\left(\sum_{m=0}^{n-1} S_m \right)^q \right] &\leq n^{q-1} \mathbb{E} \left[\sum_{m=0}^{n-1} S_m^q \right] = n^{q-1} \sum_{m=0}^{n-1} 2^{-m} \sum_{k=0}^{2^m-1} 2^{mq} |\theta_{m,k}|^p \\ &\leq 2^{q-1} n^{q-1} \left(|\theta_{0,0}|^p + \sum_{m=1}^{n-1} 2^{-m} \sum_{k=0}^{2^{m-1}-1} \left(2^m \theta_{m,2k}^2 + 2^m \theta_{m,2k+1}^2 \right)^q \right) \\ &\leq 2^{q-1} n^{q-1} \left(|\theta_{0,0}|^p + \sum_{m=1}^{n-1} \frac{1}{2} \left(\max_k (2^m \theta_{m,2k}^2 + 2^m \theta_{m,2k+1}^2) \right)^q \right) \end{aligned}$$

$$\begin{aligned}
&\leq 2^{q-1}n^{q-1}(\gamma_2(n))^q \left(|\theta_{0,0}|^p + \sum_{m=1}^{n-1} \frac{1}{2} \left(\min_k (2^m \theta_{m,2k}^2 + 2^m \theta_{m,2k+1}^2) \right)^q \right) \\
&\leq 2^{q-1}n^{q-1}(\gamma_2(n))^q \left(|\theta_{0,0}|^p + \sum_{m=1}^{n-1} \left(2^{-m} \sum_{k=0}^{2^{m-1}-1} (2^m \theta_{m,2k}^2 + 2^m \theta_{m,2k+1}^2) \right)^q \right) \\
&= 2^{q-1}n^{q-1}(\gamma_2(n))^q \sum_{m=0}^{n-1} \mathbb{E}[S_m]^q \\
&\leq 2^{q-1}n^{q-1}(\gamma_2(n))^q \left(\sum_{m=0}^{n-1} \mathbb{E}[S_m] \right)^q.
\end{aligned}$$

Selecting $\varrho_p(n) := 2^{p/2-1}n^{p/2-1}(\gamma_2(n))^{p/2}$, we thus get

$$\mathbb{E} \left[\left(\sum_{m=0}^{n-1} S_m \right)^q \right] \leq \varrho_p(n) \left(\sum_{m=0}^{n-1} \mathbb{E}[S_m] \right)^q = \varrho_p(n) s_n^p.$$

For $0 < q < 1$, an analogous reasoning as above yields that

$$\mathbb{E} \left[\left(\sum_{m=0}^{n-1} S_m \right)^q \right] \geq n^{q-1} 2^{q-1} (\gamma_2(n))^{-q} \sum_{m=0}^{n-1} \mathbb{E}[S_m]^q \geq \frac{1}{\varrho_p(n)} s_n^p,$$

where $\varrho_p(n) := n^{1-p/2} 2^{1-p/2} (\gamma_2(n))^{p/2}$. This establishes the lower bound in the reverse Jensen condition. \square

Our next goal is to prove Proposition 4.6, which is the key result for all remaining proofs. The proof of Proposition 4.6 will in turn be based on the following lemma.

Lemma 6.1. *For $n \in \mathbb{N}$ and $m \leq n-1$, if t is a dyadic rational number in $[0, 1)$ with binary expansion $t = \sum_{j=1}^n 2^{-j} a_j$ for $a_j \in \{0, 1\}$, we have $e_{m,k}(t + 2^{-n}) - e_{m,k}(t) = 2^{m/2-n} (1 - 2a_{m+1}) \mathbb{1}_{\{\lfloor 2^m t \rfloor = k\}}$.*

Proof. For $m \leq n-1$ and $\psi := \mathbb{1}_{[0,1/2)} - \mathbb{1}_{[1/2,1)}$, we have

$$e_{m,k}(t + 2^{-n}) - e_{m,k}(t) = 2^{-m/2} (e_{0,0}(2^m t + 2^{m-n} - k) - e_{0,0}(2^m t - k)) = 2^{m/2-n} \psi(2^m t - k), \quad (6.1)$$

Furthermore, it follows that

$$\begin{aligned}
\psi(2^m t - k) &= \psi \left(\sum_{j=1}^n 2^{m-j} a_j - k \right) = \psi \left(\sum_{j=m+1}^n 2^{m-j} a_j - \left(k - 2^m \sum_{j=1}^m 2^{-j} a_j \right) \right) \\
&= \psi \left(\frac{1}{2} a_{m+1} + \sum_{j=m+2}^n 2^{m-j} a_j - (k - \lfloor 2^m t \rfloor) \right).
\end{aligned}$$

As $k - \lfloor 2^m t \rfloor \in \mathbb{Z}$ and $\sum_{j=m+1}^n 2^{m-j} a_j \in [0, 1)$, we have $\psi(2^m t - k) \neq 0$ if and only if $\lfloor 2^m t \rfloor = k$. Furthermore, since $\sum_{j=m+2}^n 2^{m-j} a_j \in [0, 1/2)$ and $a_{m+1}/2 \in \{0, 1/2\}$, we must have

$$\psi \left(\frac{1}{2} a_{m+1} + \sum_{j=m+2}^n 2^{m-j} a_j \right) = \psi \left(\frac{1}{2} a_{m+1} \right) = 1 - 2a_{m+1}.$$

Hence, $\psi(2^m t - k) = (1 - 2a_{m+1}) \mathbb{1}_{\{k = \lfloor 2^m t \rfloor\}}$. Substituting this identity back into (6.1) completes the proof. \square

Proof of Proposition 4.6. For $n \in \mathbb{N}$, let the n^{th} truncation of x be given by

$$x_n(t) = \sum_{m=0}^{n-1} \sum_{k=0}^{2^m-1} \theta_{m,k} e_{m,k}(t).$$

Since the Faber-Schauder functions $e_{m,k}$ vanish on $\{k2^{-n} : k = 0, \dots, 2^n\}$ for $m \geq n$, we have $x(k2^{-n}) = x_n(k2^{-n})$ for $k = 0, \dots, 2^n$. Using the fact that R_n is uniformly distributed on $\{k2^{-n} : k = 0, \dots, 2^n - 1\}$ and Lemma 6.1, we get

$$\begin{aligned} V_n^{(p)} &= 2^n \mathbb{E} \left[|x_n(R_n + 2^{-n}) - x_n(R_n)|^p \right] \\ &= 2^n \mathbb{E} \left[\left| \sum_{m=0}^{n-1} \sum_{k=0}^{2^m-1} \theta_{m,k} (e_{m,k}(R_n + 2^{-n}) - e_{m,k}(R_n)) \right|^p \right] \\ &= 2^n \mathbb{E} \left[\left| \sum_{m=0}^{n-1} 2^{m/2-n} \sum_{k=0}^{2^m-1} \theta_{m,k} (1 - 2U_{m+1}) \mathbb{1}_{\{k=2^m R_m\}} \right|^p \right] \\ &= 2^{n(1-p)} \mathbb{E} \left[\left| \sum_{m=0}^{n-1} 2^{m/2} \theta_{m,2^m R_m} (1 - 2U_{m+1}) \right|^p \right] = 2^{n(1-p)} \mathbb{E} \left[\left| \sum_{m=0}^{n-1} Y_m \right|^p \right], \end{aligned} \quad (6.2)$$

where $Y_m := 2^{m/2} \theta_{m,2^m R_m} (1 - 2U_{m+1})$ for $m \in \mathbb{N}_0$. Let $\mathcal{F}_0 := \{\emptyset, \Omega\}$ and $\mathcal{F}_n := \sigma(U_1, \dots, U_n)$ for $n \in \mathbb{N}$. Since U_1, U_2, \dots, U_n can be uniquely recovered from R_n , we also have $\mathcal{F}_n = \sigma(R_n)$. As $(1 - 2U_m)$ defines an i.i.d. sequence of symmetric random variables, and $\theta_{m,2^m R_m}$ is \mathcal{F}_m -measurable, thus $X_n = \sum_{m=0}^{n-1} Y_m$ is an (\mathcal{F}_n) -martingale. Therefore, the Burkholder inequality implies the existence of constants $0 < A_p \leq B_p < \infty$ depending only on p such that

$$A_p 2^{n(1-p)} \mathbb{E} \left[\left(\sum_{m=0}^{n-1} Y_m^2 \right)^{p/2} \right] \leq V_n^{(p)} \leq B_p 2^{n(1-p)} \mathbb{E} \left[\left(\sum_{m=0}^{n-1} Y_m^2 \right)^{p/2} \right]. \quad (6.3)$$

Moreover, as $|1 - 2U_{m+1}| = 1$, we have

$$Y_m^2 = (2^{m/2} \theta_{m,2^m R_m})^2 (1 - 2U_{m+1})^2 = 2^m \theta_{m,2^m R_m}^2 = S_m. \quad (6.4)$$

This completes the proof of (4.3) for arbitrary $p > 1$. In the case $p = 2$, the martingale differences (Y_m) clearly satisfy $\mathbb{E}[\sum_{m=0}^{n-1} Y_m^2] = \mathbb{E}[(\sum_{m=0}^{n-1} Y_m^2)^2]$, which yields (6.4) by way of (6.2), (6.3), and (6.4). \square

Proof of Theorem 2.5. We start by proving the “only if” direction and assume that the function x admits the Hurst roughness exponent H . We must prove that $\xi_n \rightarrow 1 - H$. For any $p > 1/H \geq 1$, Proposition 4.6 and condition (4.6) yield that there exists $A_p > 0$ such that

$$A_p 2^{n(1-p+p\xi_n - \log_2 \varrho_p(n)/n)} = A_p \varrho_p^{-1}(n) 2^{n(1-p)} s_n^p = A_p \varrho_p^{-1}(n) 2^{n(1-p)} \mathbb{E} \left[\sum_{m=0}^{n-1} S_m \right]^{p/2} \leq V_n^{(p)}.$$

Since $\limsup_n V_n^{(p)} = 0$, we must thus have $\limsup_n \xi_n < 1 - 1/p$. Sending $p \downarrow 1/H$ now gives $\limsup_n \xi_n \leq 1 - H$. In the same way, one proves that $\liminf_n \xi_n \geq 1 - H$.

To prove the “if” direction, let us assume that $\lim_n \xi_n = \xi$. This then yields

$$\lim_{n \uparrow \infty} n \left(1 - p + p\xi_n \pm \frac{1}{n} \log_2 \varrho_p(n) \right) = \begin{cases} +\infty & \text{if } p > (1 - \xi)^{-1}, \\ -\infty & \text{if } p < (1 - \xi)^{-1}. \end{cases}$$

Applying condition (4.6) to (4.3) and taking $n \uparrow \infty$ implies that $\lim_n V_n^{(p)} = \infty$ for $p > (1 - \xi)^{-1}$ and $\lim_n V_n^{(p)} = 0$ for $p < (1 - \xi)^{-1}$; Therefore, we must have $H = 1 - \xi$. This completes the proof. \square

Proof of Proposition 2.6. Let $(B_t^H)_{t \in [0,1]}$ denote a fractional Brownian motion with Hurst parameter H , defined on the filtered probability space $(\tilde{\Omega}, (\mathcal{G}_t), \mathcal{G}, \mathbb{Q})$. Then the Faber–Schauder coefficients of the sample paths,

$$\theta_{m,k} = 2^{m/2} \left(2X_{\frac{2k+1}{2^{m+1}}} - X_{\frac{k}{2^m}} - X_{\frac{k+1}{2^m}} \right),$$

form a sequence of centered normal random variables on the probability space $(\tilde{\Omega}, \mathcal{G}, \mathbb{Q})$.

Now consider the probability space $(\Omega, \mathcal{F}, \mathbb{P})$ supporting the random variable $\{R_m\}$ from (4.2). Then $\{S_m\}_{m \in \mathbb{N}_0} = \{2^m \theta_{m, 2^m R_m}^2\}_{m \in \mathbb{N}_0}$ is a sequence of random variables defined on the product space $(\Omega \times \tilde{\Omega}, \mathcal{F} \otimes \mathcal{G}, \mathbb{P} \otimes \mathbb{Q})$. According (4.6), we must show that for every $p > 0$, with \mathbb{Q} -probability one, there exists a subexponential function ϱ_p and $n_p \in \mathbb{N}$ such that for $n \geq n_p$,

$$\frac{1}{\varrho_p(n)} \mathbb{E} \left[2^{2n(H-1)} \sum_{m=0}^{n-1} S_m \right]^{p/2} \leq \mathbb{E} \left[\left(2^{2n(H-1)} \sum_{m=0}^{n-1} S_m \right)^{p/2} \right] \leq \varrho_p(n) \mathbb{E} \left[2^{2n(H-1)} \sum_{m=0}^{n-1} S_m \right]^{p/2}, \quad (6.5)$$

where the notation \mathbb{E} denotes as usual the expectation with respect to \mathbb{P} . To this end, we note that \mathbb{Q} -a.s. as $n \uparrow \infty$,

$$\mathbb{E} \left[2^{2n(H-1)} \sum_{m=0}^{n-1} S_m \right]^{p/2} = \left(2^{n(2H-1)} 2^{-n} \sum_{m=0}^{n-1} \sum_{k=0}^{2^m-1} \theta_{m,k}^2 \right)^{p/2} = (2^{n(2H-1)} V_n^{(2)})^{p/2} \rightarrow 1, \quad (6.6)$$

where the second identity follows from Lemma 1.1 (ii) in [7] and the convergence from Gladyshev's theorem [9].

On the other hand, Proposition 4.6 states that

$$\frac{2^{n(pH-1)} V_n^{(p)}}{B_p} \leq \mathbb{E} \left[\left(2^{2n(H-1)} \sum_{m=0}^{n-1} S_m \right)^{p/2} \right] \leq \frac{2^{n(pH-1)} V_n^{(p)}}{A_p}. \quad (6.7)$$

As observed by Rogers [21], the self-similarity of fractional Brownian motion implies that

$$2^{n(pH-1)} V_n^{(p)} = 2^{n(pH-1)} \sum_{k=0}^{2^n-1} |B_{(k+1)2^{-n}}^H - B_{k2^{-n}}^H|^p \sim 2^{-n} \sum_{k=0}^{2^n-1} |B_{k+1}^H - B_k^H|^p, \quad (6.8)$$

where \sim means equality in law. In particular, the \mathbb{Q} -expectation of the $Y_n := 2^{n(pH-1)} V_n^{(p)}$ is bounded from above by a finite constant c , uniformly in n . It follows that $\mathbb{Q}[Y_n > n^2] \leq c/n^2$, and a Borel–Cantelli argument yields that $Y_n \leq n^2$ for sufficiently large n , \mathbb{Q} -a.s. In conjunction with (6.7) and (6.6), this establishes the right-hand inequality in (6.5) with $\varrho_p(n) = 2n^2/A_p$.

For the left-hand inequality, we take $q > p$ and note that by (6.8) and Jensen's inequality,

$$Y_n^{-q} \sim \left(2^{-n} \sum_{k=0}^{2^n-1} |B_{k+1}^H - B_k^H|^p \right)^{-q} \leq 2^{-n} \sum_{k=0}^{2^n-1} |B_{k+1}^H - B_k^H|^{-p/q}.$$

Since the increments $B_{k+1}^H - B_k^H$ are standard normally distributed, the \mathbb{Q} -expectations of Y_n^{-q} are also bounded from above, uniformly in n . A similar Borel–Cantelli argument as above then yields that $Y_n \geq 1/n^{2q}$ for sufficiently large n , \mathbb{Q} -a.s., and we obtain the left-hand inequality in (6.5) with $\varrho_p(n) = 2B_p n^{2q}$. Thus, both inequalities in (6.5) hold, e.g., with $\varrho_p(n) := 2(A_p^{-1} \vee B_p) n^{2(p+1)}$. \square

Proof of Proposition 4.1. To prove (a), we suppose first that $\xi > 1/2$. Since (4.4) states that $V_n^{(2)} = 2^{n(2\xi_n-1)}$ and this expression converges to infinity, we must have $H \leq 1/2$. In the same way, we get $H \geq 1/2$ if $\xi < 1/2$.

To prove (b), we take $p > 1/H \geq 2$. Applying Jensen's inequality to (6.3) gives

$$V_n^{(p)} \geq A_p 2^{n(1-p)} \mathbb{E} \left[\left(\sum_{m=0}^{n-1} S_m \right)^{p/2} \right] \geq A_p 2^{n(1-p)} \mathbb{E} \left[\left(\sum_{m=0}^{n-1} S_m \right) \right]^{p/2} = A_p 2^{n(1-p+p\xi_n)}. \quad (6.9)$$

Since $\lim_n V_n^{(p)} = 0$, we must have $1 - p + p\xi < 0$. Taking $p \downarrow 1/H$ gives $H \geq 1 - \xi$. The proof of (c) is analogous. \square

Proof of Proposition 4.2. Let us first consider the case $p \geq 2$. It follows from (6.9) that

$$V_n^{(p)} \geq A_p 2^{n(1-p)} \mathbb{E} \left[\sum_{m=0}^{n-1} S_m \right]^{p/2} = A_p 2^{n(1-p)} \left(\sum_{m=0}^{n-1} \int_0^1 \widehat{F}_m^{-1}(t) dt \right)^{p/2}.$$

Furthermore, we have

$$\int_0^1 \widehat{F}_m^{-1}(t) dt = \sum_{k=1}^{m^\nu} \int_{(k-1)/m^\nu}^{k/m^\nu} \widehat{F}_m^{-1}(t) dt.$$

Note that $2^{-m} \lfloor 2^m(k-1)/m^\nu \rfloor \leq (k-1)/m^\nu \leq k/m^\nu \leq 2^{-m} \lceil 2^m k/m^\nu \rceil$. Moreover, both $2^{-m} \lfloor 2^m(k-1)/m^\nu \rfloor$ and $2^{-m} \lceil 2^m k/m^\nu \rceil$ belong to $\{k2^{-m} : k = 0, \dots, 2^m\}$. Hence,

$$\widehat{F}_m^{-1} \left(2^{-m} \lceil \frac{2^m k}{m^\nu} \rceil \right) \geq \widehat{F}_m^{-1}(t) \geq \widehat{F}_m^{-1} \left(2^{-m} \lfloor \frac{2^m(k-1)}{m^\nu} \rfloor \right) \quad (6.10)$$

for all $t \in [(k-1)/m^\nu, k/m^\nu]$. This gives

$$V_n^{(p)} \geq A_p 2^{n(1-p)} \left[\sum_{m=0}^{n-1} \frac{1}{m^\nu} \sum_{k=1}^{m^\nu} \widehat{F}_m^{-1} \left(2^{-m} \lfloor \frac{2^m(k-1)}{m^\nu} \rfloor \right) \right]^{p/2} = A_p 2^{n(1-p-p\xi_{\nu,n}^-)}.$$

Moreover, applying Jensen's inequality to (4.3), we get

$$V_n^{(p)} \leq B_p 2^{n(1-p)} n^{p/2} \mathbb{E} \left[\left(\frac{1}{n} \sum_{m=0}^{n-1} S_m \right)^{p/2} \right] \leq B_p 2^{n(1-p)} n^{p/2-1} \sum_{m=0}^{n-1} \mathbb{E}[S_m^{p/2}].$$

We once again apply (6.10) to this inequality and obtain

$$\begin{aligned} V_n^{(p)} &\leq B_p 2^{n(1-p)} n^{p/2-1} \left(\sum_{m=0}^{n-1} \frac{1}{m^\nu} \sum_{k=1}^{m^\nu} \left[\widehat{F}_m^{-1} \left(2^{-m} \lceil \frac{2^m k}{m^\nu} \rceil \right) \right]^{p/2} \right) \\ &\leq B_p 2^{n(1-p)} n^{(\nu+1)(p/2-1)} \sum_{m=0}^{n-1} \frac{1}{m^\nu} \sum_{k=1}^{m^\nu} \left[\widehat{F}_m^{-1} \left(2^{-m} \lceil \frac{2^m k}{m^\nu} \rceil \right) \right]^{p/2} \\ &\leq B_p 2^{n(1-p)} n^{(\nu+1)(p/2-1)} \left[\sum_{m=0}^{n-1} \frac{1}{m^\nu} \sum_{k=1}^{m^\nu} \widehat{F}_m^{-1} \left(2^{-m} \lceil \frac{2^m k}{m^\nu} \rceil \right) \right]^{p/2} \\ &= B_p 2^{n(1-p+p\xi_{\nu,n}^+ + (\nu+1)(p/2-1) \log_2 n/n)}. \end{aligned}$$

Moreover, a similar inequality can be obtained for $1 \leq p \leq 2$,

$$A_p 2^{n(1-p+p\xi_{\nu,n}^- + (\nu+1)(p/2-1) \log_2 n/n)} \leq V_n^{(p)} \leq B_p 2^{n(1-p+p\xi_{\nu,n}^+)}.$$

In both cases ($p \geq 2$ or $1 \leq p \leq 2$), the exponents inside the brackets converge to $1 - p + p\xi_\nu^\pm$ as $n \uparrow \infty$. Therefore $\lim_n V_n^{(p)} = \infty$, for $p < (1 - \xi_\nu^-)^{-1}$. For $p > (1 - \xi_\nu^-)^{-1}$, we have $\lim_n V_n^{(p)} = 0$. This leads to $1 - \xi_\nu^+ \leq H \leq 1 - \xi_\nu^-$, and concludes the proof. \square

Proof of Proposition 4.3. (a): It follows from Proposition 4.6 that there exists $B_1 > 0$ such that

$$V_n^{(1)} \leq B_1 \mathbb{E} \left[\left(\sum_{m=0}^{n-1} S_m \right)^{1/2} \right] \leq B_1 \left(\sum_{m=0}^{n-1} \mathbb{E}[S_m] \right)^{1/2} = B_1 s_n.$$

Therefore, $\sup_n V_n^{(1)} \leq B_1 \sup_n s_n < \infty$, and $\sup_n V_n^{(1)}$ coincides with the total variation of the continuous function x (see, e.g., Theorem 2 in §5 of Chapter VIII in [20]).

(b): Following from Proposition 4.6, we have

$$A_1 \left(2^{-n/2} \sum_{k=0}^{2^n-1} |\theta_{n,k}| \right) = A_1 \mathbb{E}[S_n^{1/2}] \leq A_1 \mathbb{E} \left[\left(\sum_{m=0}^{n-1} S_m \right)^{1/2} \right] \leq V_n^{(1)},$$

for some $A_1 > 0$. Taking suprema on both sides completes our proof. \square

Proof of Proposition 4.4. We first prove that the statement holds if $|\mu_{m,k}| \geq |\theta_{m,k}|$ for $0 \leq m \leq \nu - 1$ and $k \leq 2^m - 1$. To this end, let us make the dependence of the p^{th} variation (2.1) and the random variables in (4.2) on the underlying function explicit by writing $V_n^{(p)}(x)$ and $V_n^{(p)}(y)$ as well as $(S_m^x)_{m \in \mathbb{N}}$ and $(S_m^y)_{m \in \mathbb{N}}$ for x and y , respectively. It is clear that $S_m^x = S_m^y$ for $m \geq \nu$ and $S_m^y \geq S_m^x$ for $m \leq \nu - 1$. By Proposition 4.6, for $p \geq 1$ and $n \geq \nu$, there exists $0 < A_p \leq B_p$ such that

$$\begin{aligned} V_n^{(p)}(y) &\leq B_p 2^{n(1-p)} \mathbb{E} \left[\left(\sum_{m=0}^{n-1} S_m^y \right)^{p/2} \right] = B_p 2^{n(1-p)} \mathbb{E} \left[\left(\sum_{m=0}^{\nu-1} (S_m^y - S_m^x) + \sum_{m=0}^{n-1} S_m^x \right)^{p/2} \right] \\ &\leq B_p 2^{n(1-p)} (2^{p/2-1} \vee 1) \left(\mathbb{E} \left[\left(\sum_{m=0}^{\nu-1} (S_m^y - S_m^x) \right)^{p/2} \right] + \mathbb{E} \left[\left(\sum_{m=0}^{n-1} S_m^x \right)^{p/2} \right] \right) \\ &\leq B_p 2^{n(1-p)} (2^{p/2-1} \vee 1) \mathbb{E} \left[\left(\sum_{m=0}^{\nu-1} (S_m^y - S_m^x) \right)^{p/2} \right] + \frac{B_p}{A_p} (2^{p/2-1} \vee 1) V_n^{(p)}(x). \end{aligned}$$

Moreover, as $S_m^y \geq S_m^x$ for $m \geq 0$,

$$V_n^{(p)}(y) \geq A_p 2^{n(1-p)} \mathbb{E} \left[\left(\sum_{m=0}^{n-1} S_m^y \right)^{p/2} \right] \geq A_p 2^{n(1-p)} \mathbb{E} \left[\left(\sum_{m=0}^{n-1} S_m^x \right)^{p/2} \right] \geq \frac{A_p}{B_p} V_n^{(p)}(x).$$

Since $\mathbb{E}[(\sum_{m=0}^{\nu-1} S_m^y - S_m^x)^{p/2}] < \infty$, we get for $p \geq 1$,

$$\frac{A_p}{B_p} \limsup_{n \uparrow \infty} V_n^{(p)}(x) \leq \limsup_{n \uparrow \infty} V_n^{(p)}(y) \leq \frac{(2^{p/2-1} \vee 1) B_p}{A_p} \limsup_{n \uparrow \infty} V_n^{(p)}(x),$$

and this inequality is also valid if we replace \limsup with \liminf . Thus, it follows from Proposition 2.3 that the function y admits the Hurst roughness exponent H if and only if the function x admits the Hurst roughness exponent H .

For arbitrary Faber-Schauder coefficients $(\theta_{m,k})$ and $(\mu_{m,k})$, we consider a function h with Faber-Schauder coefficients $(\eta_{m,k})$ such that $\eta_{m,k} = |\theta_{m,k}| + |\mu_{m,k}|$ for $m \leq \nu - 1$ and $\eta_{m,k} = |\theta_{m,k}|$ for $m \geq \nu$. Hence, the function x admits the Hurst roughness exponent H if and only if the function h admits the Hurst roughness exponent H , and if and only if the function y admits the Hurst roughness exponent H . This completes the proof. \square

Proof of Proposition 4.5. It suffices to prove Proposition 4.5 with $\nu = 0$; for $\nu \geq 1$, the result holds due to Proposition 4.4. Let us denote $\sigma_{m,k} := \theta_{m,k}/|\theta_{m,k}|$, then $\sigma_{m,k} \in \{-1, +1\}$ and $\mu_{m,k} = \sigma_{m,k}|\mu_{m,k}|$. Using that $x + y$ has the Faber-Schauder coefficients $(\theta_{m,k} + \mu_{m,k})$ and applying Jensen's inequality to (6.3) yields,

$$\begin{aligned}
V_n^{(p)}(x + y) &\leq B_p 2^{n(1-p)} \mathbb{E} \left[\left(\sum_{m=0}^{n-1} 2^m (|\theta_{m,2^m R_m}| + |\mu_{m,2^m R_m}|)^2 \sigma_{m,k}^2 \right)^{p/2} \right] \\
&= B_p 2^{n(1-p)} \mathbb{E} \left[\left(\sum_{m=0}^{n-1} 2^m (|\theta_{m,2^m R_m}| + |\mu_{m,2^m R_m}|)^2 \right)^{p/2} \right] \\
&\leq B_p 2^{n(1-p)+p/2} \mathbb{E} \left[\left(\sum_{m=0}^{n-1} 2^m |\theta_{m,2^m R_m}|^2 + \sum_{m=0}^{n-1} 2^m |\mu_{m,2^m R_m}|^2 \right)^{p/2} \right] \\
&\leq B_p 2^{n(1-p)+p/2} (2^{p/2} \vee 1) \left(\mathbb{E} \left[\left(\sum_{m=0}^{n-1} 2^m \theta_{m,2^m R_m}^2 \right)^{p/2} \right] + \mathbb{E} \left[\left(\sum_{m=0}^{n-1} 2^m \mu_{m,2^m R_m}^2 \right)^{p/2} \right] \right) \\
&\leq \frac{B_p}{A_p} (2^p \vee 2^{p/2}) (V_n^{(p)}(x) + V_n^{(p)}(y)).
\end{aligned}$$

Here we have used again the notation $V_n^{(p)}(\cdot)$ introduced in the proof of Proposition 4.4. Similarly, we have

$$V_n^{(p)}(x + y) \geq \frac{A_p}{B_p} (1 \wedge 2^{p/2}) (V_n^{(p)}(x) + V_n^{(p)}(y)).$$

Passing to the limit $n \uparrow \infty$ thus yields the result. \square

6.2 Proofs for the results in Section 3

Proof of Theorem 3.3. We prove (a) and (b) together. Fix $x \in C[0, 1]$. For $\lambda > 0$ we write $\phi := \log_2 \lambda$ and we will minimize (3.3) and (3.4) over ϕ rather than over λ . Recall from (3.2) that

$$\widehat{H}_k(2^\phi x) = \widehat{H}_k(x) - \frac{\phi}{k}. \quad (6.11)$$

One therefore sees that the objective functions in (3.3) and (3.4) are strictly convex in ϕ , and so minimizers can be computed as the unique zeros of the corresponding derivatives. Differentiating the objective function in (3.3) and summing by parts gives

$$\begin{aligned}
&\frac{1}{2} \frac{\partial}{\partial \phi} \sum_{k=n-m}^n \alpha_{n-k} \left(\widehat{H}_k(2^\phi x) - \widehat{H}_{k-1}(2^\phi x) \right)^2 \\
&= c_n^s \phi + \sum_{k=n-m}^n \frac{\alpha_{n-k}}{k(k-1)} (\widehat{H}_k(x) - \widehat{H}_{k-1}(x)) \\
&= c_n^s \phi + \widehat{H}_n(x) \frac{\alpha_0}{n(n-1)} + \sum_{k=n-m}^{n-1} \widehat{H}_k(x) \left(\frac{\alpha_{n-k}}{k(k-1)} - \frac{\alpha_{n-k-1}}{(k+1)k} \right) - \widehat{H}_{n-m-1}(x) \frac{\alpha_m}{(n-m)(n-m-1)}.
\end{aligned} \quad (6.12)$$

Setting this expression equal to zero yields the global minimizer ϕ_n^s ,

$$\phi_n^s = -\frac{1}{c_n^s} \left(\frac{\widehat{H}_n(x)}{n} \cdot \frac{\alpha_0}{n-1} + \sum_{k=n-m}^{n-1} \frac{\widehat{H}_k(x)}{k} \left(\frac{\alpha_{n-k}}{k-1} - \frac{\alpha_{n-k-1}}{k+1} \right) - \frac{\widehat{H}_{n-m-1}(x)}{n-m-1} \cdot \frac{\alpha_m}{n-m} \right).$$

Applying (6.11) to $\hat{H}_n(2^{\phi_n^s}x)$ yields the asserted expression for the sequential scale estimator. The proof for the terminal scale estimator is analogous. The assertion for the regression scale estimator follows by standard computations for linear regression.

(c) For $\eta > 0$, we have

$$\arg \min_{\lambda > 0} \sum_{k=n-m}^n \alpha_{n-k} \left(\hat{H}_k(\lambda \eta x) - \hat{H}_{k-1}(\lambda \eta x) \right)^2 = \frac{1}{\eta} \arg \min_{\lambda > 0} \sum_{k=n-m}^n \alpha_{n-k} \left(\hat{H}_k(\lambda x) - \hat{H}_{k-1}(\lambda x) \right)^2 = \frac{\lambda_n^s}{\eta},$$

where λ_n^s is the sequential scaling factor. Therefore, $H_n^s(\eta x) = \hat{H}_n(\lambda_n^s x) = H_n^s(x)$. The same argument yields the scale invariance of the terminal and regression scale estimators.

(d) First, we consider the sequential scale estimator. Using (6.12) one sees that $\sum_k \beta_{n,k} = 1$ so that

$$H_n^s - H = \beta_{n,n}(\hat{H}_n - H) + \cdots + \beta_{n,n-m-1}(\hat{H}_{n-m-1} - H).$$

Since $\beta_{n,n-k} = O(n)$ for each k , the assertion follows. The proof for the terminal scale estimator is analogous. For the regression scale estimator, one checks that $\frac{1}{c^r} \sum_{k=0}^m \alpha_k(n-k)(k-a) = 1$ and proceeds as before. \square

Proof of Proposition 3.6. Since the minimization problems in (3.5) and (3.7) admit unique solutions for every function $x \in C[0, 1]$, it suffices to show (3.5) is equivalent to (3.7) when taking the above parameters. Let $\lambda = 1/\sqrt{b_2}$, and we rewrite optimization problem in (3.7) into

$$\begin{aligned} & \arg \min_{h \in \mathbb{R}, b_q > 0} \sum_{k \in \mathcal{K}} \left(\log_2 m(2, k, n) - \log_2 b_2 - 2h(\log_2 k - n) \right)^2 \\ &= \arg \min_{h \in \mathbb{R}, b_q > 0} \sum_{j=0}^m \left((j-n) + \log_2 V_{n-j}^{(2)} - \log_2 b_2 - 2h(j-n) \right)^2 \\ &= \arg \min_{h \in \mathbb{R}, \lambda > 0} \sum_{j=0}^m \left(2(j-n) + 2\log_2 s_{n-j} + 2\log_2 \lambda - 2h(j-n) \right)^2 \\ &= \arg \min_{h \in \mathbb{R}, \lambda > 0} \sum_{j=0}^m \left((n-j) \left(1 - \frac{\log_2 s_{n-j}}{n-j} \right) - \log_2 \lambda - h(n-j) \right)^2 \\ &= \arg \min_{h \in \mathbb{R}, b_q > 0} \sum_{j=0}^m \alpha \cdot \left((n-j)(\hat{H}_{n-j}(x) - h) - \log_2 \lambda \right)^2, \end{aligned}$$

where the second inequality follows from [18, Proposition 2.1]. This completes the proof. \square

Proof of Theorem 3.8. We only prove (a) and (b) together for sequential scale estimates; an analogous argument yields the same result for terminal scale estimates. We again take $\phi = \log_2 \lambda$ and minimize (3.8) and (3.9) over ϕ rather than λ . Differentiating (3.8) and summing by parts yields

$$\begin{aligned} & \frac{1}{2} \frac{\partial}{\partial \phi} \sum_{j=1}^N \sum_{k=n-m}^n \alpha_{n-k} \left(\hat{H}_k(2^\phi x_{\tau_j}) - \hat{H}_{k-1}(2^\phi x_{\tau_j}) \right)^2 \\ &= N c_n^s \phi + \sum_{j=1}^N \sum_{k=n-m}^n \frac{\alpha_{n-k}}{k(k-1)} (\hat{H}_k(x_{\tau_j}) - \hat{H}_{k-1}(x_{\tau_j})) = c_n^s \left(N \phi - \sum_{j=1}^N \log_2 \lambda_n^{s, \{\tau_j\}} \right). \end{aligned}$$

Since the objective functions in (3.8) and (3.9) are also strictly convex in ϕ , then setting the rightmost argument equal to zero gives the global minimizer $\phi_n^* := \log_2 \lambda_n^{s, \mathbb{T}} = \sum_{j=1}^N \log_2 \lambda_n^{s, \{\tau_j\}} / N$. Then (6.11) directly gives the representation of $H_n^{s, \mathbb{T}}$. The assertion (c) follows directly from (c) in Theorem 3.3, and this completes the proof. \square

Data availability statement. The financial data used in this paper was purchased from FirstRate Data. The authors are willing to share the data upon request within the limitations posed by the service agreement with FirstRate Data.

References

- [1] Rama Cont and Purba Das. Quadratic variation and quadratic roughness. *arXiv preprint arXiv:1907.03115*, 2019.
- [2] Rama Cont and Purba Das. Functions with quadratic variation along refining partitions. *arXiv preprint arXiv:2109.12635*, 2021.
- [3] Rama Cont and Nicolas Perkowski. Pathwise integration and change of variable formulas for continuous paths with arbitrary regularity. *Trans. Amer. Math. Soc. Ser. B*, 6:161–186, 2019.
- [4] Hans. Föllmer. Calcul d’Itô sans probabilités. In *Seminar on Probability, XV (Univ. Strasbourg, Strasbourg, 1979/1980)*, volume 850 of *Lecture Notes in Math.*, pages 143–150. Springer, Berlin, 1981.
- [5] Hans Föllmer. Probabilistic aspects of financial risk. In *European Congress of Mathematics, Vol. I (Barcelona, 2000)*, volume 201 of *Progr. Math.*, pages 21–36. Birkhäuser, Basel, 2001.
- [6] Hans Föllmer and Alexander Schied. Probabilistic aspects of finance. *Bernoulli*, 19(4):1306–1326, 2013.
- [7] Nina Gantert. Self-similarity of Brownian motion and a large deviation principle for random fields on a binary tree. *Probab. Theory Related Fields*, 98(1):7–20, 1994.
- [8] Jim Gatheral, Thibault Jaisson, and Mathieu Rosenbaum. Volatility is rough. *Quantitative Finance*, 18(6):933–949, 2018.
- [9] E. G. Gladyshev. A new limit theorem for stochastic processes with Gaussian increments. *Teor. Veroyatnost. i Primenen*, 6:57–66, 1961.
- [10] Tilmann Gneiting and Martin Schlather. Stochastic models that separate fractal dimension and the Hurst effect. *SIAM review*, 46(2):269–282, 2004.
- [11] Xiyue Han, Alexander Schied, and Zhenyuan Zhang. A limit theorem for Bernoulli convolutions and the ϕ -variation of functions in the Takagi class. *arXiv preprint arXiv:2102.02745*, 2021.
- [12] Xiyue Han, Alexander Schied, and Zhenyuan Zhang. A probabilistic approach to the Φ -variation of classical fractal functions with critical roughness. *Statist. Probab. Lett.*, 168:108920, 2021.
- [13] Harold Edwin Hurst. Long-term storage capacity of reservoirs. *Transactions of the American society of civil engineers*, 116(1):770–799, 1951.
- [14] Kestutis Kubilius. private communication. 2021.
- [15] Kestutis. Kubilius and Dmitriy. Melichov. On the convergence rates of Gladyshev’s Hurst index estimator. *Nonlinear Anal. Model. Control*, 15(4):445–450, 2010.
- [16] Kestutis Kubilius, Yuliya Mishura, and Kostiantyn Ralchenko. *Parameter estimation in fractional diffusion models*, volume 8. Springer, 2017.

- [17] Yuliya Mishura. *Stochastic calculus for fractional Brownian motion and related processes*, volume 1929 of *Lecture Notes in Mathematics*. Springer-Verlag, Berlin, 2008.
- [18] Yuliya Mishura and Alexander Schied. Constructing functions with prescribed pathwise quadratic variation. *J. Math. Anal. Appl.*, 442(1):117 – 137, 2016.
- [19] Yuliya Mishura and Alexander Schied. On (signed) Takagi–Landsberg functions: p th variation, maximum, and modulus of continuity. *J. Math. Anal. Appl.*, 473(1):258–272, 2019.
- [20] I. P. Natanson. *Theory of functions of a real variable*. Frederick Ungar Publishing Co., New York, 1955. Translated by Leo F. Boron with the collaboration of Edwin Hewitt.
- [21] L. C. G. Rogers. Arbitrage with fractional Brownian motion. *Math. Finance*, 7(1):95–105, 1997.
- [22] Mathieu Rosenbaum. First order p -variations and Besov spaces. *Statist. Probab. Lett.*, 79(1):55–62, 2009.
- [23] Alexander Schied and Iryna Voloshchenko. Pathwise no-arbitrage in a class of Delta hedging strategies. *Probability, Uncertainty and Quantitative Risk*, 1, 2016.
- [24] Alexander Schied and Zhenyuan Zhang. On the p th variation of a class of fractal functions. *Proc. Amer. Math. Soc.*, 148(12):5399–5412, 2020.

Appendix A Summary statistics of simulation results of scale estimators

In the following tables, the notion * indicates the estimator provides the most accurate estimate among other same type scale estimators with the same choice of α_k . The notion ** indicates the estimator provides the most accurate estimate among other same type scale estimators. The notion *** indicates the estimator provides the most accurate estimate among all scale estimators.

	Statistics of the estimator $H_{14,m}^s$							
	$m = 0$				$m = 1$			
	Mean	SD	Max	Min	Mean	SD	Max	Min
$H = 0.1$	0.099919*	0.011943	0.149813	0.056969	0.100315	0.009449	0.134374	0.067877
$H = 0.2$	0.200005*	0.010901	0.238976	0.165422	0.200025	0.008949*	0.23232	0.162269
$H = 0.3$	0.299816	0.010059	0.334461	0.261401	0.299919	0.008376*	0.327773	0.264127
$H = 0.4$	0.399893	0.009009	0.434788	0.368169	0.399951*	0.007891*	0.426723	0.371593
$H = 0.5$	0.499718	0.007884	0.526962	0.472658	0.499707	0.007109*	0.522209	0.471404
$H = 0.6$	0.599762*	0.006872	0.627094	0.575309	0.599624	0.006462*	0.621050	0.575765
$H = 0.7$	0.698706*	0.006240	0.721899	0.676534	0.698582	0.006228*	0.720322	0.675723
$H = 0.8$	0.794982*	0.006583***	0.820344	0.769845	0.793801	0.007322	0.824400	0.770167
$H = 0.9$	0.881231*	0.008394**	0.921041	0.854979	0.879373	0.009083	0.917665	0.851021
	$m = 2$				$m = 3$			
	Mean	SD	Max	Min	Mean	SD	Max	Min
	Mean	SD	Max	Min	Mean	SD	Max	Min
$H = 0.1$	0.099886	0.009424*	0.136753	0.069017	0.099936	0.010727	0.139802	0.061253
$H = 0.2$	0.200106	0.008955	0.231931	0.167398	0.199554	0.010194	0.235919	0.162845
$H = 0.3$	0.300044**	0.008571	0.335387	0.269684	0.299823	0.009470	0.333725	0.265087
$H = 0.4$	0.399876	0.008084	0.432217	0.370187	0.399538	0.009092	0.431218	0.363756
$H = 0.5$	0.499660	0.007404	0.523056	0.464010	0.499667*	0.008731	0.528883	0.466862
$H = 0.6$	0.599567	0.007014	0.627059	0.574044	0.598951	0.008342	0.631752	0.570221
$H = 0.7$	0.698007	0.007354	0.725668	0.672044	0.697265	0.008704	0.730208	0.661906
$H = 0.8$	0.792865	0.008434	0.829035	0.768428	0.791387	0.009990	0.835215	0.758630
$H = 0.9$	0.877070	0.010245	0.916485	0.843747	0.874204	0.011644	0.915458	0.834735

Table 2: Summary statistics of $H_{14,m}^s$ for $m = 0, 1, 2, 3$ and $\alpha_k = 1$, based on 5,000 sample paths of fractional Brownian motion with $H = 0.1, \dots, 0.9$.

Statistics of the estimator $H_{14,m}^s$								
	$m = 0$				$m = 1$			
	Mean	SD	Max	Min	Mean	SD	Max	Min
$H = 0.1$	0.100092	0.011873	0.150170	0.056770	0.099828	0.008547	0.127596	0.065712
$H = 0.2$	0.199776	0.011136	0.240770	0.159987	0.200043	0.008280	0.232334	0.162076
$H = 0.3$	0.300056	0.009946	0.339476	0.265604	0.299918	0.007835	0.326454	0.269939
$H = 0.4$	0.399600	0.009028	0.434175	0.360468	0.399979**	0.007155	0.430390	0.374945
$H = 0.5$	0.499804	0.007931	0.533363	0.471955	0.499882*	0.006534	0.525116	0.477588
$H = 0.6$	0.599572	0.006886	0.633219	0.573089	0.599603*	0.006046	0.620327	0.578300
$H = 0.7$	0.698641	0.006219	0.719381	0.674051	0.698661*	0.005935**	0.721704	0.678166
$H = 0.8$	0.794887*	0.006725*	0.826453	0.772112	0.794209	0.006866	0.822946	0.769846
$H = 0.9$	0.881335**	0.008244*	0.921836	0.852331	0.879925	0.008792	0.915534	0.850589
	$m = 2$				$m = 3$			
	Mean	SD	Max	Min	Mean	SD	Max	Min
$H = 0.1$	0.099876	0.007493	0.129953	0.071361	0.100071*	0.006978**	0.126737	0.075602
$H = 0.2$	0.199922	0.007099	0.227172	0.177197	0.199967*	0.006693***	0.220944	0.172895
$H = 0.3$	0.299955*	0.006780	0.320631	0.273710	0.299931	0.006539**	0.321495	0.274597
$H = 0.4$	0.399857	0.006429	0.427159	0.378889	0.399771	0.006098***	0.422200	0.378042
$H = 0.5$	0.499743	0.006066	0.522755	0.475519	0.499772	0.005923**	0.521005	0.474153
$H = 0.6$	0.599554	0.005904*	0.622810	0.573918	0.599356	0.006002	0.624153	0.578191
$H = 0.7$	0.698292	0.006231	0.721227	0.675774	0.697845	0.006549	0.724682	0.674578
$H = 0.8$	0.793779	0.007612	0.822952	0.763904	0.792982	0.008007	0.824512	0.765368
$H = 0.9$	0.878400	0.009369	0.917645	0.849337	0.877539	0.010113	0.924094	0.846662

Table 3: Summary statistics of $H_{14,m}^s$ for $m = 0, 1, 2, 3$ and $\alpha_k = 2^{-k}$, based on 5,000 sample paths of fractional Brownian motion with $H = 0.1, \dots, 0.9$.

Statistics of the estimator $H_{14,m}^s$								
	$m = 0$				$m = 1$			
	Mean	SD	Max	Min	Mean	SD	Max	Min
$H = 0.1$	0.099943	0.011934	0.147937	0.045033	0.099969**	0.008726	0.128431	0.067500
$H = 0.2$	0.199999***	0.01122	0.240132	0.156438	0.199921	0.008193	0.232569	0.167628
$H = 0.3$	0.299806	0.010252	0.341208	0.257757	0.29996*	0.007742	0.327678	0.274976
$H = 0.4$	0.399952**	0.009063	0.436843	0.364071	0.399830	0.007070	0.424741	0.377298
$H = 0.5$	0.499817	0.007948	0.527437	0.468422	0.499940**	0.006564	0.522672	0.474438
$H = 0.6$	0.599789***	0.006874	0.627419	0.574071	0.599626	0.005975	0.623829	0.574921
$H = 0.7$	0.698751**	0.006102	0.725649	0.675392	0.698574	0.005709	0.719164	0.677358
$H = 0.8$	0.795085***	0.006744*	0.822602	0.771840	0.794320	0.006839	0.826165	0.768887
$H = 0.9$	0.881241*	0.008288*	0.921585	0.855508	0.880197	0.008839	0.918558	0.854729
	$m = 2$				$m = 3$			
	Mean	SD	Max	Min	Mean	SD	Max	Min
$H = 0.1$	0.100055	0.007887	0.126905	0.068307	0.099927	0.007350*	0.129347	0.074203
$H = 0.2$	0.199901	0.007536	0.224059	0.171667	0.199996	0.006950*	0.223676	0.170429
$H = 0.3$	0.300052	0.007065	0.322451	0.274368	0.299918	0.006617*	0.326169	0.272859
$H = 0.4$	0.399907	0.006509	0.425491	0.374506	0.399846	0.006259*	0.419846	0.375931
$H = 0.5$	0.499768	0.006039	0.521730	0.478102	0.499897	0.006037*	0.518972	0.478191
$H = 0.6$	0.599625	0.005767	0.618484	0.577963	0.599397	0.005611**	0.619302	0.578627
$H = 0.7$	0.698594	0.005805*	0.722649	0.673040	0.698437	0.005929	0.720921	0.677943
$H = 0.8$	0.794060	0.007040	0.822353	0.768917	0.793841	0.007342	0.819619	0.768108
$H = 0.9$	0.879309	0.008966	0.923246	0.851958	0.878718	0.009361	0.920193	0.847680

Table 4: Summary statistics of $H_{14,m}^s$ for $m = 0, 1, 2, 3$ and $\alpha_k = 3^{-k}$, based on 5,000 sample paths of fractional Brownian motion with $H = 0.1, \dots, 0.9$.

Statistics of the estimator $H_{14,m}^t$								
	$m = 0$				$m = 1$			
	Mean	SD	Max	Min	Mean	SD	Max	Min
$H = 0.1$	0.100055	0.007887	0.126905	0.068307	0.099927	0.007350*	0.129347	0.074203
$H = 0.2$	0.199901	0.007536	0.224059	0.171667	0.199996*	0.006950*	0.223676	0.170429
$H = 0.3$	0.300052*	0.007065	0.322451	0.274368	0.299918	0.006617*	0.326169	0.272859
$H = 0.4$	0.399907*	0.006509	0.425491	0.374506	0.399846	0.006259*	0.419846	0.375931
$H = 0.5$	0.499768	0.006039	0.521730	0.478102	0.499897*	0.006037*	0.518972	0.478191
$H = 0.6$	0.599625*	0.005767	0.618484	0.577963	0.599397	0.005611*	0.619302	0.578627
$H = 0.7$	0.698594	0.005805*	0.722649	0.67304	0.698437	0.005929	0.720921	0.677943
$H = 0.8$	0.794060	0.007040	0.822353	0.768917	0.793841	0.007342	0.819619	0.768108
$H = 0.9$	0.879309	0.008966*	0.923246	0.851958	0.878718	0.009361	0.920193	0.847680
	$m = 2$				$m = 3$			
	Mean	SD	Max	Min	Mean	SD	Max	Min
$H = 0.1$	0.099990**	0.007840	0.127840	0.071984	0.099928	0.007554	0.129927	0.074316
$H = 0.2$	0.199831	0.007465	0.22323	0.169808	0.199811	0.007322	0.233022	0.173120
$H = 0.3$	0.299914	0.006980	0.325617	0.276038	0.29994	0.007169	0.329404	0.274685
$H = 0.4$	0.400106	0.006810	0.423902	0.376752	0.399900	0.006802	0.425208	0.377642
$H = 0.5$	0.499730	0.006591	0.523266	0.475371	0.499731	0.006549	0.521616	0.476157
$H = 0.6$	0.599618	0.006122	0.624828	0.575033	0.59928	0.006578	0.621621	0.574352
$H = 0.7$	0.698619*	0.005966	0.718677	0.674662	0.697668	0.007225	0.729165	0.670561
$H = 0.8$	0.794135*	0.006997*	0.826835	0.771690	0.792222	0.008799	0.828761	0.763724
$H = 0.9$	0.879758*	0.008984	0.916587	0.851504	0.876291	0.010654	0.921829	0.840577

Table 5: Summary statistics of $H_{14,m}^t$ for $m = 0, 1, 2, 3$ and $\alpha_k = 1$, based on 5,000 sample paths of fractional Brownian motion with $H = 0.1, \dots, 0.9$.

Statistics of the estimator $H_{14,m}^t$								
	$m = 0$				$m = 1$			
	Mean	SD	Max	Min	Mean	SD	Max	Min
$H = 0.1$	0.100170	0.011822	0.147589	0.055928	0.100133	0.008627	0.129959	0.068138
$H = 0.2$	0.200002**	0.011192	0.238465	0.159581	0.199851	0.008225	0.229803	0.172667
$H = 0.3$	0.299922	0.010162	0.334221	0.265097	0.299994***	0.007768	0.329271	0.269828
$H = 0.4$	0.399952	0.009125	0.436611	0.366501	0.399814	0.007137	0.425045	0.373541
$H = 0.5$	0.499913	0.007851	0.530656	0.466232	0.499917*	0.006543	0.531764	0.474092
$H = 0.6$	0.599717**	0.006918	0.623197	0.575179	0.599614	0.006034	0.621877	0.575870
$H = 0.7$	0.698894***	0.006139	0.719705	0.673920	0.698721	0.005932*	0.723822	0.671824
$H = 0.8$	0.794945*	0.006743*	0.827019	0.771502	0.794395	0.006866	0.823659	0.772892
$H = 0.9$	0.881356***	0.008060***	0.921464	0.854952	0.880021	0.008778	0.919397	0.853913
	$m = 2$				$m = 3$			
	Mean	SD	Max	Min	Mean	SD	Max	Min
$H = 0.1$	0.100139	0.007279	0.131191	0.075491	0.099913*	0.006979**	0.124624	0.074384
$H = 0.2$	0.200095	0.007184	0.227000	0.177685	0.199939	0.006705*	0.221707	0.172483
$H = 0.3$	0.300144	0.006772	0.325993	0.278375	0.299937	0.006570*	0.324022	0.276102
$H = 0.4$	0.400027**	0.006524	0.425519	0.374025	0.399889	0.006214*	0.422415	0.374863
$H = 0.5$	0.499711	0.006212	0.524966	0.475232	0.499788	0.006017*	0.521382	0.475716
$H = 0.6$	0.599510	0.005945*	0.619559	0.574051	0.599441	0.006058	0.619238	0.576311
$H = 0.7$	0.698319	0.006105	0.721827	0.675784	0.697945	0.006567	0.727214	0.674625
$H = 0.8$	0.793660	0.007434	0.829180	0.765972	0.792956	0.008055	0.831261	0.765138
$H = 0.9$	0.878840	0.009378	0.923740	0.846288	0.877205	0.010016	0.919466	0.843777

Table 6: Summary statistics of $H_{14,m}^t$ for $m = 0, 1, 2, 3$ and $\alpha_k = 2^{-k}$, based on 5,000 sample paths of fractional Brownian motion with $H = 0.1, \dots, 0.9$.

Statistics of the estimator $H_{14,m}^t$								
	$m = 0$				$m = 1$			
	Mean	SD	Max	Min	Mean	SD	Max	Min
$H = 0.1$	0.100037*	0.011728	0.140692	0.055353	0.100079	0.008730	0.128397	0.067108
$H = 0.2$	0.200128	0.011102	0.236032	0.159651	0.199828	0.008312	0.230264	0.170370
$H = 0.3$	0.299534	0.010047	0.332625	0.264458	0.300056	0.007723	0.331428	0.272270
$H = 0.4$	0.399971***	0.009106	0.431659	0.363436	0.399961	0.007094	0.429382	0.376024
$H = 0.5$	0.499992***	0.007922	0.528172	0.472384	0.500023	0.006575	0.522352	0.475980
$H = 0.6$	0.599753	0.006950	0.625720	0.576299	0.599746	0.005905	0.624144	0.576014
$H = 0.7$	0.698869*	0.006260	0.721114	0.673535	0.698649	0.005803***	0.721808	0.676645
$H = 0.8$	0.794988**	0.006651**	0.829838	0.772527	0.794475	0.006951	0.823850	0.769172
$H = 0.9$	0.881090*	0.008375*	0.916729	0.853933	0.880249	0.008823	0.925273	0.848017
	$m = 2$				$m = 3$			
	Mean	SD	Max	Min	Mean	SD	Max	Min
$H = 0.1$	0.099838	0.007592	0.127198	0.069969	0.100086	0.007054*	0.123099	0.073411
$H = 0.2$	0.199993*	0.007320	0.223722	0.174965	0.199876	0.006697**	0.226046	0.169291
$H = 0.3$	0.300044*	0.006835	0.322977	0.274827	0.299778	0.006458**	0.326765	0.274880
$H = 0.4$	0.400174	0.006437	0.422680	0.374559	0.399957	0.006183**	0.422629	0.376235
$H = 0.5$	0.499821	0.006182	0.523656	0.476170	0.499844	0.005826**	0.526166	0.477285
$H = 0.6$	0.599670*	0.005677***	0.619468	0.580369	0.599485	0.005737***	0.618901	0.579351
$H = 0.7$	0.698284	0.005941	0.720389	0.677671	0.698230	0.006165	0.719869	0.675982
$H = 0.8$	0.793913	0.007323	0.824903	0.772210	0.793449	0.007665	0.827193	0.766429
$H = 0.9$	0.879150	0.009227	0.915919	0.850454	0.878248	0.009433	0.918080	0.847491

Table 7: Summary statistics of $H_{14,m}^t$ for $m = 0, 1, 2, 3$ and $\alpha_k = 3^{-k}$, based on 5,000 sample paths of fractional Brownian motion with $H = 0.1, \dots, 0.9$.

Statistics of the estimator $H_{14,m}^r$								
	$m = 1$				$m = 2$			
	Mean	SD	Max	Min	Mean	SD	Max	Min
$H = 0.1$	0.099802	0.011821	0.147157	0.053691	0.099946	0.009167	0.136044	0.066088
$H = 0.2$	0.199891	0.011064	0.235855	0.160344	0.200002**	0.008663	0.229828	0.168487
$H = 0.3$	0.300159	0.010045	0.334410	0.258899	0.300061*	0.008291	0.329010	0.265592
$H = 0.4$	0.399796	0.009112	0.432658	0.364491	0.400101*	0.007638	0.427370	0.370879
$H = 0.5$	0.499733	0.008055	0.531783	0.472772	0.499851*	0.006825*	0.522664	0.472294
$H = 0.6$	0.599657	0.006846	0.625944	0.571158	0.599752*	0.006308*	0.620603	0.577184
$H = 0.7$	0.698866*	0.006217	0.721814	0.675802	0.698553	0.006124*	0.722752	0.675251
$H = 0.8$	0.795041*	0.006610*	0.826854	0.774466	0.794035	0.007124	0.821212	0.768978
$H = 0.9$	0.881147*	0.008262*	0.914492	0.853565	0.879367	0.008958	0.920190	0.850689
	$m = 3$				$m = 4$			
	Mean	SD	Max	Min	Mean	SD	Max	Min
$H = 0.1$	0.099798	0.008673*	0.131503	0.06384	0.099956*	0.008679	0.129138	0.066508
$H = 0.2$	0.200176	0.008279*	0.229783	0.171403	0.199561	0.008610	0.229358	0.163942
$H = 0.3$	0.299876	0.007869*	0.326852	0.270480	0.299756	0.008442	0.336645	0.270983
$H = 0.4$	0.400105	0.007513*	0.423819	0.369470	0.399698	0.007883	0.425872	0.373376
$H = 0.5$	0.499786	0.007120	0.525363	0.472305	0.499506	0.007578	0.528633	0.470385
$H = 0.6$	0.599616	0.006726	0.626606	0.576749	0.599229	0.007387	0.624235	0.573484
$H = 0.7$	0.698017	0.006909	0.730083	0.674721	0.697573	0.007920	0.728312	0.668374
$H = 0.8$	0.792891	0.008161	0.826811	0.765727	0.791655	0.009433	0.827390	0.755285
$H = 0.9$	0.877598	0.010010	0.925893	0.845408	0.875151	0.011188	0.916800	0.841185

Table 8: Summary statistics of $H_{14,m}^r$ for $m = 1, 2, 3, 4$ and $\alpha_k = 1$, based on 5,000 sample paths of fractional Brownian motion with $H = 0.1, \dots, 0.9$.

Statistics of the estimator $H_{14,m}^r$								
	$m = 1$				$m = 2$			
	Mean	SD	Max	Min	Mean	SD	Max	Min
$H = 0.1$	0.099937	0.011951	0.137595	0.058712	0.099999***	0.008552	0.130340	0.068743
$H = 0.2$	0.200036*	0.011120	0.246150	0.154677	0.199937	0.008163	0.229227	0.168626
$H = 0.3$	0.299890	0.010031	0.330807	0.264121	0.299929*	0.007753	0.331403	0.26215
$H = 0.4$	0.400015**	0.009119	0.433325	0.364442	0.400065	0.007144	0.425056	0.367774
$H = 0.5$	0.500031*	0.007949	0.530650	0.470520	0.499780	0.006621	0.521942	0.476402
$H = 0.6$	0.599714*	0.006830	0.624182	0.576554	0.599633	0.005929*	0.622836	0.581028
$H = 0.7$	0.698587*	0.006209	0.719516	0.671027	0.698440	0.005863*	0.718268	0.674570
$H = 0.8$	0.794808*	0.006724*	0.821365	0.770799	0.794187	0.007116	0.827266	0.769225
$H = 0.9$	0.881273**	0.008429*	0.917695	0.857595	0.879757	0.008838	0.918288	0.853700
	$m = 3$				$m = 4$			
	Mean	SD	Max	Min	Mean	SD	Max	Min
$H = 0.1$	0.099824	0.007503	0.125811	0.072737	0.099996	0.006947***	0.123928	0.076238
$H = 0.2$	0.199860	0.007287	0.227495	0.170213	0.199877	0.006852*	0.225453	0.177016
$H = 0.3$	0.299889	0.006874	0.325041	0.276084	0.299888	0.006585*	0.323135	0.273458
$H = 0.4$	0.399900	0.006584	0.426375	0.372286	0.399790	0.006410*	0.424042	0.378696
$H = 0.5$	0.499744	0.006196	0.522855	0.478300	0.499610	0.006090*	0.520806	0.474678
$H = 0.6$	0.599638	0.006006	0.620848	0.578634	0.599287	0.006148	0.623605	0.576132
$H = 0.7$	0.698226	0.006204	0.720305	0.669503	0.698023	0.006634	0.718761	0.675856
$H = 0.8$	0.793568	0.007515	0.830671	0.769333	0.792857	0.008321	0.828837	0.766465
$H = 0.9$	0.878728	0.009470	0.919576	0.844620	0.877172	0.010140	0.923151	0.841673

Table 9: Summary statistics of $H_{14,m}^r$ for $m = 1, 2, 3, 4$ and $\alpha_k = 2^{-k}$, based on 5,000 sample paths of fractional Brownian motion with $H = 0.1, \dots, 0.9$.

Statistics of the estimator $H_{14,m}^r$								
	$m = 1$				$m = 2$			
	Mean	SD	Max	Min	Mean	SD	Max	Min
$H = 0.1$	0.100020	0.011855	0.141606	0.054681	0.099839	0.008604	0.128458	0.068702
$H = 0.2$	0.199855	0.011014	0.241253	0.164065	0.199868	0.008241	0.227691	0.169139
$H = 0.3$	0.300170	0.009964	0.338734	0.263439	0.300012**	0.007708	0.331498	0.272591
$H = 0.4$	0.400059*	0.008959	0.431632	0.367075	0.399899	0.007152	0.424191	0.372004
$H = 0.5$	0.499650	0.007919	0.528892	0.470652	0.499991**	0.006446	0.521239	0.475957
$H = 0.6$	0.599739	0.006920	0.622967	0.573574	0.599745**	0.005935	0.620107	0.578733
$H = 0.7$	0.698789**	0.006104	0.721242	0.676698	0.698571	0.005853**	0.722985	0.677960
$H = 0.8$	0.795050**	0.006684**	0.828585	0.770753	0.794348	0.006876	0.824135	0.770721
$H = 0.9$	0.881272*	0.008252**	0.917566	0.852121	0.880040	0.008822	0.919397	0.851128
	$m = 3$				$m = 4$			
	Mean	SD	Max	Min	Mean	SD	Max	Min
$H = 0.1$	0.100015	0.007554	0.128338	0.069827	0.100013*	0.007099*	0.129946	0.074972
$H = 0.2$	0.200087*	0.007206	0.226820	0.172296	0.199840	0.006699**	0.224489	0.176156
$H = 0.3$	0.299946	0.006943	0.324428	0.276048	0.299743	0.006375***	0.324617	0.271239
$H = 0.4$	0.399816	0.006484	0.424622	0.373816	0.399841	0.006133**	0.421651	0.375926
$H = 0.5$	0.499824	0.006084	0.528262	0.475539	0.499680	0.005867**	0.518366	0.479002
$H = 0.6$	0.599507	0.005774**	0.620728	0.575223	0.599511	0.005778	0.621572	0.580993
$H = 0.7$	0.698393	0.005926	0.717930	0.675968	0.698231	0.006109	0.720794	0.675521
$H = 0.8$	0.793983	0.007260	0.824286	0.768969	0.793479	0.007617	0.829818	0.765769
$H = 0.9$	0.878955	0.009069	0.929305	0.852148	0.878053	0.009510	0.921836	0.843362

Table 10: Summary statistics of $H_{14,m}^r$ for $m = 1, 2, 3, 4$ and $\alpha_k = 3^{-k}$, based on 5,000 sample paths of fractional Brownian motion with $H = 0.1, \dots, 0.9$.

Appendix B Summary statistics of estimated Hurst roughness exponent of log prices of selected futures

Year	Estimated Hurst roughness exponent for selected futures					
	ES			ZN		
	Mean	Max	Min	Mean	Max	Min
2005	0.4959	0.5343	0.4555	-	-	-
2006	0.4962	0.5418	0.4230	0.4213	0.4481	0.3796
2007	0.4664	0.5483	0.3470	0.3915	0.4470	0.3457
2008	0.3656	0.4774	0.1904	0.3400	0.3961	0.2722
2009	0.3801	0.4999	0.2706	0.3704	0.4319	0.2796
2010	0.4366	0.5476	0.3023	0.4123	0.4521	0.3499
2011	0.4305	0.5439	0.2760	0.4131	0.4599	0.3340
2012	0.4803	0.5373	0.4160	0.4655	0.5133	0.4108
2013	0.5108	0.5741	0.4397	0.4554	0.5031	0.3797
2014	0.5196	0.5911	0.3976	0.4695	0.5067	0.3867
2015	0.4893	0.5794	0.3298	0.4517	0.5103	0.3846
2016	0.5056	0.6069	0.3816	0.4706	0.5201	0.4037
2017	0.5775	0.6479	0.5189	0.4966	0.5428	0.4519
2018	0.4950	0.6120	0.3421	0.5020	0.5443	0.4234
2019	0.5116	0.6276	0.3569	0.4840	0.5324	0.4196
2020	0.4350	0.6046	0.2042	0.4975	0.5606	0.3130
2021	0.5147	0.6086	0.3995	0.5044	0.5543	0.4215

Table 11: Summary statistics of the Hurst roughness exponent for the log prices of e-mini SPX futures (ES) and 10-year treasury notes futures (ZN), estimated by $H_n^{t,T}$ with $n = 11$, $m = 1$ and $\alpha_k = 2^{-k}$.

Year	Estimated Hurst roughness exponent for selected futures					
	GC			SI		
	Mean	Max	Min	Mean	Max	Min
2007	-	-	-	0.4595	0.4890	0.3223
2008	0.4010	0.4640	0.2226	0.4174	0.4938	0.3295
2009	0.4498	0.5078	0.3831	0.4509	0.4921	0.4003
2010	0.4788	0.5399	0.4227	0.4771	0.5249	0.3906
2011	0.4617	0.5396	0.3445	0.4254	0.5190	0.3093
2012	0.4951	0.5667	0.4272	0.4801	0.5361	0.4199
2013	0.4676	0.5593	0.3496	0.4705	0.5379	0.3591
2014	0.5062	0.5580	0.4293	0.5044	0.5672	0.3989
2015	0.4974	0.5461	0.4378	0.4901	0.5324	0.4523
2016	0.4936	0.5632	0.4132	0.4961	0.5490	0.4101
2017	0.5398	0.6119	0.4974	0.5375	0.5769	0.4990
2018	0.5472	0.6044	0.5016	0.5445	0.5797	0.5103
2019	0.5321	0.6014	0.4477	0.5324	0.5881	0.4398
2020	0.4595	0.5873	0.3156	0.4358	0.5565	0.2917
2021	0.4885	0.5354	0.4320	0.4710	0.5188	0.3505

Table 12: Summary statistics of the Hurst roughness exponent for the log prices of gold futures (GC) and silver futures (SI), estimated by $H_n^{t,\mathbb{T}}$ with $n = 11$, $m = 1$ and $\alpha_k = 2^{-k}$.

Year	Estimated Hurst roughness exponent for selected futures					
	FX			NQ		
	Mean	Max	Min	Mean	Max	Min
2006	0.4815	0.5368	0.3705	0.4813	0.5212	0.4396
2007	0.4776	0.5592	0.4005	0.4758	0.5402	0.3972
2008	0.3687	0.4814	0.1843	0.3910	0.4694	0.2570
2009	0.3520	0.4526	0.2115	0.4332	0.5248	0.3527
2010	0.4060	0.4767	0.2848	0.4783	0.5734	0.3646
2011	0.3908	0.4808	0.2533	0.4717	0.5693	0.3376
2012	0.4213	0.4975	0.3603	0.5101	0.5703	0.4579
2013	0.4729	0.5293	0.4148	0.5347	0.5862	0.4790
2014	0.4881	0.5487	0.4058	0.5310	0.6154	0.4274
2015	0.4560	0.5231	0.3641	0.5075	0.5925	0.3592
2016	0.4612	0.5555	0.3060	0.5181	0.6045	0.4024
2017	0.5549	0.6081	0.4968	0.5756	0.6370	0.5019
2018	0.5292	0.5852	0.4474	0.4898	0.5997	0.3632
2019	0.5615	0.6113	0.4805	0.5142	0.6456	0.3772
2020	0.4920	0.6051	0.2762	0.4441	0.6092	0.2400
2021	0.5729	0.6333	0.5189	0.5032	0.5883	0.3867

Table 13: Summary statistics of the Hurst roughness exponent for the log prices of Euro STOXX 50 futures (FX) and e-mini NASDAQ-100 futures (NQ) with $n = 11$, $m = 1$ and $\alpha_k = 2^{-k}$.

Appendix C Summary statistics of estimated Hurst roughness exponent of log volatility of selected financial indices

Estimated Hurst roughness exponent for selected indices									
Year	Index								
	AEX	BFX	BVSP	DJI	FCHI	FTSE	GDAXI	HIS	IBES
2001	0.0737	0.0459	0.0611	0.1039	0.0486	0.0604	0.0883	0.0153	0.1024
2002	0.0491	0.1044	0.0280	0.0396	0.0338	0.0724	0.0083	0.0087	0.0740
2003	0.1373	0.1383	0.1107	0.0041	0.1354	0.1230	0.0849	0.0597	0.1156
2004	0.0928	0.0744	0.1610	-0.0499	0.1070	0.0759	0.0777	0.0696	0.0808
2005	0.0697	0.0713	0.1628	0.0416	0.0985	0.0419	0.1144	0.0388	0.0803
2006	0.1242	0.0883	0.1287	0.0449	0.0809	0.1173	0.1481	0.0304	0.0761
2007	0.1196	0.0960	0.1938	0.1185	0.1148	0.1338	0.1559	0.0693	0.1185
2008	0.2032	0.1763	0.1903	0.1468	0.1991	0.1571	0.2164	0.1207	0.2092
2009	0.1573	0.1256	0.1089	0.0829	0.1482	0.0755	0.1956	0.0978	0.1696
2010	0.1416	0.1451	0.1554	0.0557	0.1410	0.0965	0.1216	0.0468	0.1721
2011	0.1904	0.1532	0.1519	0.0348	0.1573	0.0981	0.1374	0.0458	0.1847
2012	0.2091	0.1796	0.1466	0.0068	0.2130	0.0806	0.1585	0.0938	0.1830
2013	0.1220	0.0824	0.1148	0.0821	0.1401	0.0713	0.1026	0.0403	0.1292
2014	0.1024	0.1186	0.1529	0.0893	0.1071	0.0642	0.1483	0.0286	0.1416
2015	0.1622	0.1532	0.0584	0.1849	0.1438	0.1230	0.1267	0.0976	0.1157
2016	0.1406	0.1376	0.1387	0.1449	0.1495	0.0632	0.1491	0.0919	0.1445
2017	0.1359	0.1249	0.1780	0.1449	0.1335	0.0253	0.0929	-0.0153	0.1563
2018	0.1432	0.1429	0.1477	0.2150	0.0987	0.0391	0.0387	0.0543	0.1486
2019	0.0719	0.0798	0.1494	0.1858	0.0644	-0.0058	0.0369	0.0434	0.0812
2020	0.1700	0.1469	0.1304	0.1680	0.1554	0.1230	0.1467	0.1059	0.1574
2021	0.1135	0.1169	0.1937	0.1620	0.1645	0.0952	0.1507	0.1106	0.1514

Table 14: Summary statistics of the estimated Hurst roughness exponent for the log volatility of selected indices with $n = 8$, $m = 1$ and $\alpha_k = 2^{-k}$.

Estimated Hurst roughness exponent for selected indices									
Year	Index								
	IXIC	KS11	KSE	MXX	N225	SPX	SSEX	SSMI	STOXX
2001	0.1675	0.1420	0.1052	0.0822	0.0933	0.1359	0.2710	0.1056	0.0488
2002	0.0759	0.0950	0.1548	0.1053	0.1001	0.0348	0.2133	0.0907	-0.0218
2003	0.0400	0.0780	0.1745	0.0335	0.1137	0.0134	0.1631	0.1054	0.0310
2004	0.0941	0.1149	0.1711	0.0454	0.1157	-0.0121	0.1919	0.0433	0.0059
2005	0.0766	0.0668	0.1525	0.0855	0.0948	0.0575	0.1967	0.0199	0.0854
2006	0.0779	0.0706	0.1511	0.0971	0.1425	0.0734	0.1791	0.0473	0.1178
2007	0.1281	0.1355	0.1884	0.1314	0.1710	0.1445	0.1965	0.1688	0.1476
2008	0.2050	0.1696	0.2115	0.1169	0.1610	0.1792	0.1821	0.2214	0.1681
2009	0.1842	0.1655	0.2878	0.0487	0.1803	0.1358	0.1470	0.1873	0.1306
2010	0.1883	0.1434	0.1491	0.0162	0.0707	0.0960	0.1701	0.1542	0.1577
2011	0.1516	0.2000	0.1601	0.0422	0.2127	0.0867	0.0962	0.1504	0.1676
2012	0.1546	0.2130	0.1043	0.0407	0.1257	0.0003	0.0788	0.1361	0.1896
2013	0.1337	0.1003	0.1131	0.0368	0.1460	0.1006	0.0035	0.1214	0.0119
2014	0.1668	0.1054	0.0830	0.1026	0.1539	0.1439	0.0729	0.1030	-0.0033
2015	0.2673	0.1620	0.1278	0.0963	0.2100	0.2444	0.1400	0.1620	0.0864
2016	0.2638	0.0904	0.1531	0.0387	0.1739	0.2009	0.1672	0.1729	0.1000
2017	0.2056	0.0293	0.1805	0.0479	0.1352	0.2074	0.1643	0.1341	0.0664
2018	0.2178	0.0585	0.1491	0.0812	0.1232	0.2485	0.1871	0.1421	0.0136
2019	0.1913	0.0404	0.1621	0.0640	0.0979	0.2095	0.0867	0.1473	-0.0014
2020	0.1994	0.0787	0.1386	0.0689	0.0902	0.1920	0.1068	0.1754	0.1474
2021	0.1557	0.0200	0.1520	0.0317	0.1010	0.1839	0.1091	0.1762	0.0866

Table 15: Summary statistics of the estimated Hurst roughness exponent for the log volatility of selected indices with $n = 8$, $m = 1$ and $\alpha_k = 2^{-k}$.

Estimated Hurst roughness exponent for selected indices									
Year	Index								
	AEX	BFX	BVSP	DJI	FCHI	FTSE	GDAXI	HIS	IBES
2004	0.0916	0.0945	0.0907	0.0432	0.0892	0.0874	0.0677	0.0417	0.1016
2005	0.0882	0.1066	0.1083	0.0203	0.0970	0.0819	0.0759	0.0405	0.0944
2006	0.1124	0.1017	0.1431	0.0130	0.1086	0.0941	0.1177	0.0560	0.0941
2007	0.1090	0.0928	0.1664	0.0487	0.1066	0.0990	0.1313	0.0600	0.1024
2008	0.1413	0.1249	0.1762	0.1023	0.1364	0.1174	0.1639	0.0776	0.1357
2009	0.1589	0.1334	0.1630	0.1122	0.1482	0.1280	0.1825	0.0861	0.1517
2010	0.1615	0.1429	0.1675	0.1071	0.1602	0.1247	0.1796	0.0912	0.1713
2011	0.1807	0.1564	0.1622	0.0829	0.1711	0.1178	0.1741	0.0874	0.1898
2012	0.1799	0.1562	0.1460	0.0503	0.1720	0.0949	0.1579	0.0803	0.1829
2013	0.1712	0.1467	0.1479	0.0508	0.1685	0.0920	0.1335	0.0627	0.1721
2014	0.1573	0.1399	0.1464	0.0584	0.1556	0.0850	0.1400	0.0573	0.1656
2015	0.1518	0.1413	0.1276	0.0979	0.1523	0.0908	0.1376	0.0734	0.1466
2016	0.1400	0.1332	0.1207	0.1366	0.1411	0.0852	0.1354	0.0736	0.1401
2017	0.1436	0.1440	0.1406	0.1488	0.1417	0.0747	0.1335	0.0644	0.1486
2018	0.1540	0.1476	0.1399	0.1798	0.1403	0.0728	0.1087	0.0699	0.1470
2019	0.1299	0.1279	0.1604	0.1770	0.1180	0.0450	0.0887	0.0608	0.1402
2020	0.1360	0.1295	0.1581	0.1796	0.1194	0.0577	0.0893	0.0527	0.1416
2021	0.1301	0.1268	0.1595	0.1821	0.1270	0.0741	0.1000	0.0805	0.1388

Table 16: Summary statistics of the estimated Hurst roughness exponent for the log volatility of selected indices with $n = 10$, $m = 1$ and $\alpha_k = 2^{-k}$.

Estimated Hurst roughness exponent for selected indices									
Year	Index								
	IXIC	KS11	KSE	MXX	N225	SPX	SSEX	SSMI	STOXX
2004	0.1152	0.1165	0.1561	0.0787	0.1090	0.0575	0.2259	0.1059	0.0365
2005	0.0833	0.0947	0.1638	0.0781	0.1106	0.0332	0.2040	0.0865	0.0461
2006	0.0788	0.0856	0.1646	0.0721	0.1236	0.0384	0.1889	0.0684	0.0872
2007	0.1003	0.1025	0.1694	0.0972	0.1368	0.0766	0.1964	0.0872	0.1038
2008	0.1344	0.1192	0.1840	0.1159	0.1462	0.1280	0.1937	0.1372	0.1365
2009	0.1568	0.1399	0.2291	0.1049	0.1672	0.1459	0.1845	0.1659	0.1485
2010	0.1809	0.1577	0.2344	0.0862	0.1531	0.1465	0.1806	0.1867	0.1584
2011	0.1881	0.1764	0.2337	0.0627	0.1663	0.1304	0.1569	0.1819	0.1646
2012	0.1779	0.1903	0.2186	0.0415	0.1614	0.0812	0.1304	0.1647	0.1696
2013	0.1642	0.1754	0.1407	0.0371	0.1542	0.0749	0.0972	0.1510	0.1230
2014	0.1592	0.1700	0.1207	0.0598	0.1691	0.0885	0.0721	0.1394	0.0796
2015	0.1924	0.1607	0.1158	0.0819	0.1769	0.1261	0.0838	0.1500	0.0645
2016	0.2158	0.1244	0.1267	0.0754	0.1788	0.1789	0.1129	0.1534	0.0526
2017	0.2297	0.1065	0.1447	0.0741	0.1787	0.2041	0.1443	0.1569	0.0706
2018	0.2416	0.0925	0.1582	0.0703	0.1707	0.2318	0.1680	0.1673	0.0783
2019	0.2249	0.0653	0.1689	0.0622	0.1507	0.2229	0.1610	0.1586	0.0598
2020	0.2074	0.0560	0.1646	0.0676	0.1173	0.2154	0.1430	0.1619	0.0766
2021	0.1928	0.0512	0.1590	0.0684	0.1077	0.2077	0.1321	0.1688	0.0838

Table 17: Summary statistics of the estimated Hurst roughness exponent for the log volatility of selected indices with $n = 10$, $m = 1$ and $\alpha_k = 2^{-k}$.